Marine and Petroleum Geology
April 2020, Volume 114, Pages 104195 (16p.)
https://doi.org/10.1016/j.marpetgeo.2019.104195
https://archimer.ifremer.fr/doc/00599/71125/

A synthesis of the sedimentary evolution of the Demerara Plateau (Central Atlantic Ocean) from the late Albian to the Holocene

Fanget Anne-Sophie [1, *], Loncke Lies [1], Pattier France [2, 3], Marsset Tania [4], Roest Walter [2], Tallobre Cédric [5], Durrieu De Madron Xavier [1], Hernandez Molina F. Javier [6]

[1] University of Perpignan Via Domitia, Centre de Formation et de Recherche sur les Environnements Méditerranéens (CEFREM), UMR 5110, 52 Avenue Paul Alduy, 66100 Perpignan, France
[2] Institut français de recherche pour l'exploitation de la mer (Ifremer), Laboratoire Aléas géologiques et Dynamique sédimentaire - LAD, Marine Geosciences Research Unit, CS 70, 20280 Plouzané, France
[3] Service Géologique de Nouvelle-Calédonie (DIMENC), 1 ter rue Unger, BP M2 – 98849, Noumea Cedex, New Caledonia
[4] Institut français de recherche pour l'exploitation de la mer (Ifremer), Laboratoire Géodynamique et enregistrement Sédimentaire – LGS, Marine Geosciences Research Unit, CS 70, 20280 Plouzané, France
[5] University Littoral Côte d'Opale, UMR 8187, LOG, Laboratoire d'Océanologie et de Géosciences, F 62 930, Wimereux, France
[6] Department of Earth Sciences, Royal Holloway University of London, Surrey TW20 0EX, UK

* Corresponding author : Anne-Sophie Fanget, email address : annesophie.fanget@gmail.com

Abstract :

The Demerara Plateau, off the French Guiana and Surinam margin, corresponds to a prominent sub-horizontal marginal plateau. The interpretation of a large set of seismic data acquired along the Demerara Plateau and integration with previous seismic stratigraphy and drill studies enables a better understanding of the sedimentary evolution of the outer Demerara marginal plateau. Since the end of the transform activity (late Albian), three sedimentary evolutionary stages have been identified. 1) The Pre-contourite Stage (late Albian to early Miocene) is strongly controlled by the structure of the margin that influences the distribution pattern of post-transform deposits through differential thermal subsidence between transform and divergent segments. 2) The Transitional Stage (middle Miocene to early Pliocene) is expressed as a current-controlled erosive surface resulting from the onset of bottom-current interactions due to the establishment and strengthening of the modern thermohaline circulation that is coeval with the progressive closure of the Isthmus of Panama. 3) The Contourite Stage (middle Pliocene to Holocene) is characterized by the development of a contourite depositional system that is linked to the activity of the North Atlantic Deep Water circulation and by a complex interaction between alongslope and downslope processes. Our study highlights that marginal plateaus might be particularly prone to develop contourite features since they regionally influence ocean current dynamics in guiding and accelerating bottom contour currents. Marginal plateaus should thus be considered as a key target to study bottom current dynamics and paleocirculation patterns.

Highlights

► The post-transform sedimentation of the Demerara marginal plateau (DP) is studied. ► A strong relation between topography, downslope and alongslope processes shapes DP. ► Marginal plateaus are particularly prone to develop contourite deposits.

Keywords : Marginal plateau, Demerara Plateau, contourite, bottom currents, mass transport deposits, Atlantic Ocean

1. Introduction

The Demerara Plateau has long been a rather under-explored bathymetric high off French Guiana and Surinam despite its key tectonic and oceanographic position between the Cretaceous Equatorial Atlantic and the Jurassic Central Atlantic oceans. Renewed attention began with ODP expedition 207, with a drilling program dedicated to the evolution of Cretaceous to Paleocene paleoceanographic conditions in the Equatorial Atlantic gateway (Erbacher et al., 2004; Mosher et al., 2007). In parallel, an important part of the Demerara Plateau was explored through a series of industry and academic geophysical campaigns dedicated to a better knowledge of its tectonic (Basile et al., 2013; Greenroyd et al., 2007; Greenroyd et al., 2008; Loncke et al., 2009; Mercier de Lépinay 2016) and sedimentary evolution (Loncke et al., 2016; Tallobre et al., 2016; Tallobre et al., 2019). These investigations revealed the predominance of Mass Transport Deposits (MTDs) on the outer Demerara Plateau (Loncke et al., 2009). Pattier et al. (2013) published a first mapping and relative chronology of these MTDs based on the existing 6-channel seismic reflection profiles. A series of at least twelve MTDs have deposited on the outer plateau since the upper Albian. Later on, additional geophysical data of better resolution and core data enabled the discovery of contourite deposits on the outer Demerara Plateau (IGUANES cruise, Loncke et al., 2016; Tallobre et al., 2016; Tallobre et al., 2019). These contourites are thought to be related to the North Atlantic Deep Water that flows parallel to the Demerara Plateau. Loncke et al. (2016) suggest in a general paper presenting the preliminary results of these higher-resolution acquisitions that contourites might have initiated during Miocene times. In their study, Tallobre et al. (2016; 2019) focused on the recent sediment records (i.e. the last 150 000 years) associated with these contourite deposits of high paleoceanographic interest.

Thus, different datasets of diverse quality evidenced MTDs and contourites along the outer Demerara Plateau and discussed their relative age and relationships. These observations have never been synthesized in detail and integrated into a common regional stratigraphic framework.

In this work, we gather and synthetize all available data partly presented in former works in a common stratigraphic chart in order to determine the successive sedimentary stages of the Demerara Plateau from the upper Albian to the Holocene and to better constrain the apparition of contourites along the Demerara Plateau. We also discuss the geological and

oceanographic factors that control the passage from one sedimentary stage to another on the Demerara Plateau.

2. Geological setting and oceanography

2.1. Geological setting

The Demerara Plateau, part of the Surinam-French Guiana passive margin, is located at the western edge of the Equatorial Atlantic Ocean, close to the junction with the Central Atlantic Ocean (Fig. 1). The formation and evolution of the Demerara Plateau are closely linked to the opening history of the Atlantic Ocean. Prior to break-up, the Demerara Plateau was connected to the Guinea Plateau off the West African margin (Benkhelil et al., 1995; Mascle et al., 1986). The opening of the Central Atlantic Ocean during Jurassic times first structured the western edge of the Demerara Plateau as a divergent, probably volcanic margin, segment (Gouyet, 1988; Unternehr et al., 1988; Reuber et al., 2016). At the end of the early Cretaceous, the opening of the Equatorial Atlantic Ocean, in a strike-slip regime along a main transform zone, led to the break-up of the French-Guiana margin from the West African margin and to the separation of the Demerara and Guinean plateaus (Gouyet, 1988; Greenroyd et al., 2008; Unternehr et al., 1988). The eastern edge of the Demerara Plateau then formed as a divergent segment, while its northern edge formed as a transform segment. Tectonic activity ceased during the late Albian and the transform margin became passive (Basile et al., 2013; Gouyet, 1988).

The Demerara Plateau thus corresponds to a marginal plateau that derives from a complex and polyphase opening history of the Atlantic Ocean (Mercier de Lépinay et al., 2016). As a result, the Demerara Plateau exhibits a structurally controlled seafloor morphology. It consists of a prominent sub-horizontal (slope angle ranging from 1 to 3°; Pattier et al., 2013) marginal plateau (ca. 340 km long, 220 km wide) that is located between the shelf break and upper slope break at water depths ranging from ca. 120 m to 1450 m (Fig. 2) (Mercier de Lépinay et al., 2016). Based on slope values observed in bathymetric data, three main physiographic domains can be identified within the Demerara Plateau (Pattier et al., 2013): (1) the upper plateau (slope value of ca. 1°), (2) the intermediate plateau (slope value of ca. 3°), and (3) the lower plateau (slope value of ca. 1°). The transition between the upper and intermediate plateau is characterized by the presence of a major linear NW-SE

slope failure headscarp that forms an abrupt incision visible in the bathymetry (Fig. 2) (Loncke et al., 2009; Loncke et al., 2016; Pattier et al., 2013). Northward, the transition between the lower plateau and the abyssal plain is characterized by a steep and erosive continental slope (average slope value of 15°; Pattier et al., 2013) typical of narrow transform ocean-continent transitions. On the western and eastern edges of the Demerara Plateau, at the transition between the lower plateau and the abyssal plain, divergent-derived continental slopes are gentler (average slope value of 4°; Pattier et al., 2013).

Regionally, the Demerara Plateau is bordered by two major sedimentary sources: the Amazon River to the south-east and the Orinoco River to the west (Fig. 1). The Amazon and Orinoco rivers are respectively the largest and the third-largest rivers in the world in terms of water discharge (Milliman and Meade, 1983; Meade, 1994). Nevertheless, the Demerara Plateau is located far from the Amazon and Orinoco sedimentary sources and in a highstanding position with regard to the Amazon and Orinoco deep-sea sediment deposits (Fig. 1). The direct inputs of the Amazon and Orinoco rivers are thus thought to have a minimal influence on Demerara Plateau sedimentation.

Locally, the Demerara Plateau is surrounded by two main smaller rivers: the Maroni River, at the French Guiana-Surinam border, and the Oyapock River, at the French Guiana-Brazil border (Fig. 1). The Maroni River is the largest river of this region and could potentially be the main source of sediment to the Demerara Plateau. It drains a catchment area of ca. 64 230 km² and has a mean annual water discharge of ca. 1700 m^3s^{-1} (Sondag et al., 2010). The Oyapock River drains a basin area of ca. 24 630 km² and presents a lower mean annual water discharge with values close to ca. 830 m^3s^{-1} (Sondag et al., 2010).

2.2. Characteristics of water masses

Previous studies emphasize that the interaction of highly active oceanographic processes with the seafloor is an essential characteristic of the Demerara Plateau (e.g. Ingram et al., 2011; Loncke et al., 2016; Tallobre et al., 2016). Regionally, the study area is under the influence of three water masses that are part of the thermohaline circulation:

- The Antarctic Intermediate Water (AAIW), formed in the southern ocean (Peterson and Stramma, 1991; Tsuchiya et al., 1994), flows from the SE towards the NW at a

water depth of ca. 550 to 1200 m. The AAIW is characterized by a velocity of ca. 20 cm s^{-1} near 400 m water depth and by reduced velocity near the bottom layer (i.e. 5 cm s^{-1} at ca. 1000 m water depth) (Peterson and Stramma, 1991; Suga and Talley, 1995).

- The North Atlantic Deep Water (NADW), consisting of cold and salty water masses derived from the Greenland and Labrador seas, is orientated NW-SE and circulates between ca. 1200 and 4200 m water depth (Johns et al., 1993; Mauritzen et al., 2002). The NADW shows velocities generally bracketed between 20 and 29 cm s^{-1}.
- The colder and less saline Antarctic Bottom Water (AABW), formed in the Weddell and Ross seas off Antarctica, flows from the SE to the NW at a water depth deeper than ca. 4200 m (Johns et al., 1993; Mauritzen et al., 2002). The AABW is characterized by higher velocities with values reaching up to 45 cm s^{-1}.

Locally, Koltermann et al. (2011) highlight that the Demerara marginal plateau is under the influence of the AAIW and the NADW (Fig. 3). The upper plateau is directly influenced by the AAIW, while the intermediate and lower plateaus are under the influence of the NADW. The transition between the NADW and the AABW is located within the continental rise that separates the marginal plateau from the abyssal plain.

2.3. Review of previous studies

The stratigraphy of the sedimentary units of the Demerara Plateau (Fig. 4) is known from well investigations derived from hydrocarbon exploration (Gouyet, 1988; Mercier de Lépinay et al., 2016) and from ODP Expedition 207 drillings (Erbacher et al., 2004; Mosher et al., 2007). Sedimentary cover along the Demerara Plateau was deposited above an upper Albian regional unconformity (called reflector R4; Pattier et al., 2013; Pattier et al., 2015) that marks the end of the transform activity and corresponds to a sub-aerial erosive surface covered by shell debris that caps deformed upper Cretaceous and older rocks (Gouyet, 1988; Pattier et al., 2013). Post-Albian sedimentation consists of a sedimentary basin made of thick prograding wedges (up to 4 km in thickness on the continental shelf) that progressively thin seawards (Gouyet, 1988). The distal parts of the lower marginal plateau are considered to be sediment starved at present (Mosher et al., 2007; Pattier et al., 2013). Upper Cretaceous sediments record a major transgression, which includes the deposition of Cenomanian-

Turonian black shales (organic-rich laminated sediments) that overlay Albian shallow-water siliciclastic sediments (Mosher et al., 2007). Early Campanian sediments have not been recovered on the western edge of the Demerara Plateau, and the upper Campanian yields glauconite-rich horizons highlighting reduced sedimentation rates (Mosher et al., 2007). The cessation of black shale sedimentation, as well as reduced deposition rates and hiatuses, are linked to changes in oceanographic conditions that follow the opening of the Equatorial Atlantic gateway (Friedrich and Erbacher, 2006). Sedimentation on the Demerara Plateau changed from hemipelagic to pelagic by the late Campanian. At that time, fully oxic conditions were established (Mosher et al., 2007). Maastrichtian to Oligocene sediment succession at the Demerara Plateau consists of pelagic deep marine nannofossil and foraminiferal chalks and oozes deposited in an upper bathyal setting (Mosher et al., 2007). This succession records the lithological consequences of the Cretaceous/Tertiary boundary (called reflector R3; Pattier et al., 2013; Pattier et al., 2015) and the abrupt global warming associated with the Paleocene/Eocene boundary (called reflection R2; Pattier et al., 2013; Pattier et al., 2015). Due to a major erosional event that occurred in the middle Miocene (corresponding to reflector R1; Pattier et al., 2013; Pattier et al., 2015), Oligocene and even Eocene sediments on the Demerara Rise are often reworked and/or reduced in thickness (Ingram et al., 2011; Mosher et al., 2007). Finally, as a probable result of the onset of the Amazon River (and probably the Maroni River), the Pliocene sediments are clay-rich. Late Pleistocene and Holocene series are characterized by very low sedimentation rates in the distal part of the Demerara Plateau (Erbacher et al., 2004; Ingram et al., 2011; Mosher et al., 2007; Pattier et al., 2013).

Despite low sedimentation rates, recent investigations highlight that the intermediate and lower part of the Demerara Plateau has been particularly affected by slope instabilities since the Oligocene (Gaullier et al., 2010; Ingram et al., 2011; Loncke et al., 2009; O'Regan and Moran, 2007; Pattier et al., 2013). Submarine landslides (mass transport complex) pile up for a thickness of nearly 500 m in the intermediate and lower plateaus (Pattier et al., 2013). The last large MTD that is well identified on seismic data seems to have occurred during the late Miocene or early Pliocene (LM/EP MTD, Pattier et al., 2013; Pattier et al., 2015; Tallobre et al., 2016, Fig. 4). These submarine landslides are associated with a major slope failure headscarp (ca. 350 km in length) still visible on bathymetric data (Fig. 2 and zoom A). This slope failure headscarp is parallel to the transform border, suggesting a strong structural control (Loncke et al., 2009; Pattier et al., 2013; Pattier et al., 2015). Bottom current activity clearly plays an active role in middle Pliocene to Holocene sedimentation (post LM/EP MTD,

Fig. 4) by allowing the development of a contourite depositional system in the intermediate and lower plateaus (Loncke et al., 2016; Tallobre et al., 2016). This contourite depositional system is directly associated with the influence of the NADW circulation that also forms elongated seafloor depressions (e.g. furrows) and longitudinal bedforms that parallel the current (Fig. 2) (Tallobre et al., 2016). Pattier et al. (2015) also describe an enigmatic post LM/EP MTD unconformity in the upper plateau that forms sub-circular depressions. The origin of this unconformity is still debated and could be interpreted either as an erosional surface associated with bottom currents or as paleo-hydrate pockmarks (Pattier et al., 2015).

Most of the studies carried out until now focus on sedimentary processes (e.g. contourites, instabilities) and the huge available dataset has never been presented in a synthetic way with a common stratigraphic framework. Seismic stratigraphy has also never been carried out at the scale of the outer Demerara plateau. Thus, the regional Albian to Quaternary isopach and isodepth maps have never been published. Note also that contourites have been present on the intermediate and lower plateau since at least middle Pliocene-Holocene times (Loncke et al., 2016). Nevertheless, the onset and conditions of these contourite deposits were not constrained.

3. Data and Methods

The present study is based on the integration, analysis, and interpretation of seismic data acquired during both the GUYAPLAC and IGUANES cruises (Fig. 1). The GUYAPLAC cruise (2003) was carried out onboard the R/V *"L'Atalante"*. 6-channel seismic reflection profiles were acquired during this cruise. The IGUANES cruise (2013) was carried out onboard the R/V "*L'Atalante*". 24-channel and 72-channel seismic reflection profiles were acquired during the IGUANES cruise. A quality control of navigation and seismic data was first performed. Then, SEGD data were converted to SEGY, and binning, stacking and post-stack depth migration were performed. The maximum vertical resolution of seismic data is 10 m and 4 m for the 24-channel acquisition and high-resolution 72-channel acquisition, respectively. FG02 reflection seismic data acquired by FUGRO were also used in this study. Interpretations by Pattier et al. (2015) of the shallowest parts of the FG02 seismic data were made available by TOTAL S.A.

Seismic stratigraphic analysis followed basic criteria described by Payton (1977), Hardage (1987) and Emery and Myers (1996). The seismic discontinuities and units described in the

following sections were defined on the basis of the nomenclature from Basile et al. (2013) and Pattier et al. (2013; 2015), which provides correlation with the G2 industrial well (Gouyet, 1988) and the ODP Leg 207 drillings (Fig. 1) (Mosher et al., 2007). These authors identified four main discontinuities (named R4 to R1, from the oldest to the youngest) and three main seismic units (named seismic unit C, B and A, from the oldest to the youngest) along the Demerara Plateau and proposed a general chronological framework for these discontinuities and seismic units (Fig. 4). The chronological framework of these studied main discontinuities and seismic units is summarized below. The basal discontinuity R4 that separates the pre- and syn-transform sediments from the post-transform sediments is late Albian in age (Gouyet, 1988). The first post-transform seismic unit (i.e. seismic unit C) is made of upper Cretaceous sediments. Within this seismic unit, four reflections (named C4 to C1) were identified by Pattier et al. (2015). Reflections C4 and C3 are Cenomanian in age, while reflections C2 and C1 are attributed to the base of the Turonian and the base of the Maastrichtian, respectively (Pattier et al., 2015). Note that in the present study, reflection C3, which is located within the Cenomanian deposits, has not been studied due to its low-amplitude reflection. Reflections C4, C2 and C1 were studied on the IGUANES seismic data. Unfortunately, the overall low-amplitude reflection of reflections C4, C2 and C1 does not allow any detailed descriptions of these reflections and sub-units. Discontinuity R3, which separates seismic unit C from seismic unit B, correlates with the Cretaceous/Tertiary boundary (Erbacher et al., 2004; Mosher et al., 2007; Pattier et al., 2015). Seismic unit B encompasses Paleocene (seismic unit B2) and Eocene to early Miocene sediments (seismic unit B1). The transition between the Paleocene and Eocene is marked by seismic discontinuity R2 (Pattier et al., 2015). Finally, seismic unit A, which is limited at its base by a middle Miocene discontinuity R1 (Gouyet, 1988; Ingram et al., 2011), has deposited since the late Miocene (Pattier et al., 2015; Tallobre et al., 2016). Within this unit, Pattier et al. (2015) defined an important unconformity (named Uc) only visible on the upper plateau. The origin of this Uc unconformity is still debated (paleo-hydrate pockmarks? Contourite related unconformity?).

In this paper, we use the same nomenclature and stratigraphic framework described above, but we present more regional and detailed descriptions of the post-transform seismic surfaces and units. In particular, we computed new isopach maps of the post transform seismic units, hypothesizing a mean seismic velocity of 2000 m s^{-1}. We also newly describe and focus on the most recent seismic unit A (with the newly described reflections A7 to A1).

During the GUYAPLAC and IGUANES cruises, bathymetric data were also acquired using an EM 12 and EM 122 multibeam echosounder, respectively (Fig. 1). Multibeam data were processed using Ifremer CARAIBES software. Erroneous bathymetric soundings were removed. Raw data were filtered and interpolated, enabling the construction of a 25 m horizontal resolution grid. Slope gradients were calculated on the basis of this grid. Bathymetric data acquired during the recent DRADEM (onboard the R/V "*Pourquoi pas*?") and MARGATS (onboard the R/V *"L'Atalante"*) cruises in 2016, as well as the HOMONIM digital elevation model provided by the SHOM, were also integrated into the project. All data were imported in the QGIS geographic information software for compilation and analysis. All maps have been projected in UTM zone 22 N in the WGS84 geodetic system.

Oceanographic information along the Demerara Plateau is from WOCE section A20 (Koltermann et al., 2011). Data were acquired during the 316N151_3 cruise onboard the R/V Knorr in 1997. Stations 71 to 95 have been selected and imported to Ocean Data View (Schlitzer, 2017) to illustrate the distribution pattern of the main water masses along the Demerara Plateau.

Note that the term "contourite" used in this paper refers to sediments deposited or substantially reworked by the persistent action of bottom currents (e.g. Rebesco, 2005; Rebesco and Camerlenghi, 2008; Stow et al., 2002). The criteria used in the present study to identify contourites and bottom-current related features follow the concepts proposed by Faugères et al. (1999), Stow and Faugères (2008), Nielsen et al. (2008) and Rebesco et al. (2014).

4. Results

4.1. Late Albian to middle Miocene deposits

The basal discontinuity of post-transform deposits, named reflection R4, corresponds to the upper Albian unconformity (Gouyet, 1988) that separates the folded and tilted Jurassic and lower Cretaceous formations from the sub-horizontal or seaward tilted post-transform formations (i.e. late Albian to Quaternary sediments). The isodepth map of reflection R4 shows that this surface gently deepens on the upper plateau domain (Fig. 5A). One depression

has been mapped on the central part of the upper plateau (visible on seismic profile of Fig. 6 and labelled “zone 1” in Fig. 5A). On the eastern edge of the upper plateau, a bulge could be mapped (“zone 2”, Fig. 5A). At the transition between the upper plateau and the intermediate plateau, reflection R4 deepens more abruptly towards the northeast (Figs. 7, 8 and 9). Reflection R4 corresponds to an erosive surface (e.g. Figs. 6 and 7). On seismic images, reflection R4 is characterized by a high-amplitude reflection (Fig. 6), except on the lower part of the intermediate plateau and on the lower plateau, where R4 is characterized by a low-amplitude reflection and is more difficult to follow (Fig. 7).

Above reflection R4, Cenomanian to late Cretaceous seismic unit C is moderately reflective and displays an important lateral variability, with alternating low- and high-amplitude reflections and alternating continuous and discontinuous internal reflections. On the upper plateau, the lower part of seismic unit C is characterized by acoustically semi-transparent seismic facies with faint sub-parallel reflections (Figs. 6 and 7). The upper part of seismic unit C is marked by higher-amplitude reflections. Seismic unit C onlaps onto the R4 unconformity. The dip angle of internal reflections of seismic unit C is generally low on the upper plateau, except near the depression area of reflection R4 (Fig. 6). At the transition between the upper plateau and the intermediate plateau, internal reflections of seismic unit C dip seaward at a higher angle (Figs. 7, 8 and 9), following the shape of reflection R4. At the base of seismic unit C, seaward dipping clinoforms developed. They are characterized by gently seaward-dipping moderate-amplitude reflections (e.g. Fig. 7C). On the Demerara Plateau, clinoforms are restricted to the central area of the intermediate plateau, between ca. 4 to 4.7 s twtt in depth. Within seismic unit C, three reflections (named C4, C2 and C1 by Pattier et al. (2015)) have been identified and associated with minor discontinuities. Clinoforms observed on the intermediate plateau are bounded by reflection C4 that is Cenomanian in age. Reflections C4, C2 and C1 can only be picked on the upper plateau. Indeed, on the intermediate plateau, seismic unit C is affected by a large slide complex (MTD 01 in Pattier et al., 2015) that removed those series. The basal shear surface of MTD 01 affects reflections C4 to C1, as highlighted by the presence of erosional truncations (Figs. 7 and 8). Thus, the isopach map of the upper Cretaceous seismic unit C is limited to the upper plateau (Fig. 5B). On the central area of the upper plateau, sediment thickness reaches a maximum of ca. 800 m along a NW-SE axis (Fig. 5B, zone 1). On the eastern edge of the upper plateau, seismic unit C progressively thickens seaward to reach a maximum thickness of ca. 1400 m near the upper/intermediate plateau transition (Fig. 5B).

The upper boundary of seismic unit C (late Cretaceous in age), called discontinuity R3 (Fig. 4), is generally characterized by high-amplitude reflections. On the upper plateau, reflection R3 displays an overall irregular morphology that mimics the morphology of reflection R4 (Figs. 5C and 6). At the transition between the upper plateau and the intermediate plateau, reflection R3 is characterized by a seaward inflexion (Figs. 6 and 8), and then dips progressively seaward (Figs. 6 and 8). On the intermediate plateau, reflection R3 is disrupted by the presence of a MTD (labeled MTD 02 in Pattier et al., 2015; e.g. Figs. 7 and 9). Reflection R3 is characterized by the erosional truncation of the underlying upper Cretaceous deposits (seismic unit C) and is thus considered as an erosive surface.

Seismic unit B (Paleocene to Miocene in age) is divided into two sub-units called seismic units B2 and B1. Seismic unit B2 onlaps on reflection R3 (Fig. 6). Seismic unit B2 is characterized by high-amplitude reflections and is bounded by reflection R2, which marks the boundary between Paleocene and Eocene deposits. Discontinuity R2 is characterized by moderate- to high-amplitude reflection. On the upper plateau, reflection R2 displays an irregular morphology and dips gently seaward (Figs. 5E and 6). At the transition between the upper and intermediate plateau, reflection R2 is affected by a major failure headscarp and thus cannot be followed on the intermediate plateau, which corresponds to a destabilized complex area (e.g. Figs. 6, 7 and 8). Reflection R2 is an erosive surface marked by the erosional truncation of the underlying Paleocene deposits (seismic unit B2). Seismic unit B1 onlaps on reflection R2 and is highly faulted, forming a polygonal fault interval (Fig. 6). The distribution of seismic unit B is represented by both the isopach maps of Paleocene (between reflections R3 and R2; seismic unit B2; Fig. 5D) and Eocene/early Miocene deposits (i.e. seismic unit B1, Fig. 5F) and is limited to the upper plateau due to the presence of the MTDs (i.e. MTD 01 and MTD 02) that destabilized the sedimentary cover of the intermediate plateau, as mentioned before. On the upper plateau, the depocenter of Paleocene deposits (seismic unit B2), reaching a maximum thickness of ca. 200 m, is aligned along a NW-SE axis (Fig. 5D, zone 1). The depocenter of Eocene/early Miocene deposits (seismic unit B1) reaches a maximum thickness of ca. 400 m and is aligned along the same axis (Fig. 5F).

In the study area, the upper boundary of seismic unit B corresponds to reflection R1, which formed during the middle Miocene. It corresponds to an overall planar surface dipping very gently seaward (e.g. Figs. 6, 7 and 10A). Discontinuity R1 is characterized by high-amplitude reflection and is also highly affected by polygonal faults (Fig. 6). At the transition between the upper plateau and the intermediate plateau, reflection R1 is truncated by the presence of a major failure headscarp (Figs. 6, 7, 8 and 9). Due to the presence of a large

MTD (late Miocene/early Pliocene (LM/EP) MTD, see the following section) on the intermediate plateau, reflection R1 cannot be identified further seaward. Reflection R1 is characterized by the erosional truncation of the underlying deposits (i.e. seismic unit B2) and is interpreted as an erosive surface.

4.2. Late Miocene to Holocene deposits

Seismic unit A composes the most recent unit of the Demerara Plateau. Unit A rests on regional erosional surface R1 described previously (e.g. Fig. 6).

The base of seismic unit A is characterized by the presence of a deposit that shows an internally chaotic facies corresponding to the LM/EP MTD (Fig. 4, colored in yellow, Figs. 6, 7, 8 and 9). In some cases, some sparse reflections were able to be identified within this deposit (Fig. 7B). This acoustically chaotic deposit shows an irregular and erosive base and a generally rippled top (Fig. 9B). In the western part of the Demerara Plateau, this LM/EP MTD is absent or very thin (zone 1, Fig. 10B). On the eastern part of the Demerara Plateau, it is well expressed, especially on the intermediate plateau where it reaches a maximum thickness of ca. 200 m (zone 2, Fig. 10B). On the upper plateau, this LM/EP MTD rests on the erosional surface R1 (Fig. 6). On the intermediate plateau, it partly erodes older MTDs (e.g. MTDs 01 and 02 described previously). Locally, on the intermediate plateau, the LM/EP MTD outcrops (Fig. 8C) and elongated depressions develop at the top of this MTD (Figs. 2B, and “Furrows” indicated on Fig. 8C).

Above the LM/EP MTD, seismic unit A displays generally continuous and high-amplitude reflections. Within this unit, seven main reflections (named A7 to A1, from the base of the unit to the top) were distinguished at the scale of the Demerara Plateau (Fig. 4).

On the upper plateau, A7 to A1 gently dip seaward (Fig. 7). On the upper and intermediate plateau, reflections A7 to A1 form a slightly prograding sequence. The presence of an unconformity, named Uc by Pattier et al. (2015), is observed on the entire upper plateau (in red, Figs. 6 and 7A and 7B). This unconformity consists of a series of sub-circular valleys of short extent. The base of these valleys roots on erosional reflection R1 or on top of the LM/EP MTD (Figs. 6 and 7). Unconformity Uc affects reflections A7 to A5, while reflections A4 to A1 are not truncated by Uc (Fig. 7B). Rarely, smaller depressions (pockmark-like seabed features) affect reflections A7 to A2 on the upper plateau.

At the transition between the upper and intermediate plateau, seismic reflections are vertically shifted due to the presence of a prominent bathymetric headscarp (e.g. Figs. 2A, 6 and 8). This main headscarp truncates reflections R2 and R1 and affects reflections A7 to A4 (e.g. Fig. 8B). Reflections A3 to A1 are not laterally interrupted, but they mimic the shape of the headscarp (e.g. Fig. 8B).

On the intermediate plateau, seismic unit A progressively thins seawards and reflections A7 to A1 onlap the outcropping LM/EP MTD (e.g. Figs 8A and 8C). Reflections A7 to A4 are especially difficult to follow to the edge of the LM/EP MTD since they are disrupted by the presence of small paleo-depressions (Fig. 8C). Upslope-migrating sediment waves affect reflections A5 to A1 (e.g. Figs. 7B and 8A). Seismic unit A finally reappears on the lower part of the intermediate plateau, close to the transition with the lower plateau on some seismic profiles (Fig 8). There, seismic unit A onlaps the LM/EP MTD and reaches 0.5 s twtt in thickness, forming a sort of isolated distal recent sedimentary patch.

Finally, on the western edge of the intermediate plateau, the presence of three acoustically chaotic deposits (post LM/EP MTD and named MTD 04, MTD 05, and MTD 06) is observed near the main failure headscarp (Figs. 8 and 9). MTD 04 corresponds to a small and thin MTD observed locally above reflection A6 (Fig. 8). MTD 05 reaches ca. 100 ms twtt in thickness and affects reflections A7 to A2 over a large extent (ca. 35 km in length) (Fig. 9). MTD 06 is localized near the main failure headscarp and is the most recent MTD to affect Demerara Plateau sedimentation (i.e. reflection A7).

The isopach map of seismic unit A illustrates very well that the thickness of unit A is variable along the Demerara Plateau (as shown in Fig. 10C). Unit A reaches a maximum thickness of ca. 700 m on the upper plateau and thins down to ca. 350 m until the slope failure headscarp (zone 1, Fig. 10C). Except along small patchy accumulations that are elongated in a NW-SE direction, sediment thickness decreases progressively to zero meters downslope of the main failure headscarp to ca. 2800 m of water depth. This ca. 30 km wide depleted zone roughly parallels the NW-SE main failure headscarp (zone 2, Fig. 10C). From ca. 2800 to ca. 3600 m of water depth, sediment thickness increases again but in a patchy way, forming roughly NW-SE elongated accumulations that drastically thicken towards the SE (reaching up to 550 meters near the divergent border of the Demerara Plateau) (zone 3, Fig. 10C). Another depleted zone is observed below 3600 m of water depth, where sediment thickness reaches ca.

zero meters at the transition between the intermediate plateau and the lower plateau (zone 4, Fig. 10C).

5. Interpretation and discussion

5.1. Evolutionary stages of the Demerara Marginal Plateau

Based on the analysis of seismic data, three distinct evolutionary stages that are either controlled by structural inheritance, differential subsidence or bottom-current processes have been identified: (1) the Pre-contourite Stage, which formed from the late Albian to early Miocene and includes seismic units C and B previously described; (2) the Transitional Stage, from the middle Miocene to early Pliocene, which is characterized by the main erosive surface R1 and by the presence of the major LM/EP gravitational event; and (3) the Contourite Stage, which formed during middle Pliocene-Holocene times and is made of seismic unit A. These three stages are discussed below.

5.1.1. Pre-contourite stage: late Albian to early Miocene deposits

During this first stage, no clear influence of bottom-current processes has been observed. Post-transform sediments rest on a regional erosive surface (reflection R4) that is late Albian in age and marks the end of the transform activity (Gouyet, 1988). This unconformity sealed more than 8 km of pre- and syn-transform sediment series deformed as a result of transform motion (Basile et al., 2013; Mercier de Lépinay et al., 2016). Erosion of these series by the striking angular R4 unconformity is related to a late Albian uplift of the Demerara Plateau and indicates that during this time most of the plateau was emerged or under the influence of shallow marine processes (Basile et al., 2013; Gouyet, 1988; Greenroyd et al., 2008; Mosher et al., 2007). The late Albian unconformity is characterized on the upper plateau by an irregular depth (Figs. 5A and 6, depression along zone 1 and global seaward inflection on the lower plateau). This variation in depth of reflection R4 could be related to a differential subsidence of the Demerara Plateau due to former tectonic segmentation (Loncke et al., 2016) or to loading of the adjacent abyssal plains by the Amazon fan. Zone 2 forms a local elevation of reflection R4. It corresponds to a deep anticline that was not totally peneplained during the

erosional event that occurred during the upper Albian (Mercier de Lépinay et al., 2016; Pattier et al., 2013).

Following the end of the transform activity, the first post-transform sediments (i.e. seismic unit C, Fig. 4) that are late Cretaceous in age deposited on the Demerara Plateau following a major transgression (Erbacher et al., 2004; Mosher et al., 2007). Basal reflections of seismic unit C onlap the upper Albian surface and infill inherited depressions. Unit C clearly thickens from the upper plateau towards the intermediate plateau (Fig. 5B).

At the base of seismic unit C, prior reflection C4, small-scale clinoforms have been identified and preserved on the intermediate plateau (Fig. 7). Clinoforms are recognized as ubiquitous deltaic, shallow marine and continental margin depositional morphologies (Cattaneo et al., 2007; Patruno et al., 2015). On the Demerara Plateau, these small-scale clinoforms are restricted to the central area of the intermediate plateau and to the base of seismic unit C. Drillings of Leg ODP 207 indicate that the base of seismic unit C (i.e. late Albian sediments) consists of shallow water siliciclastic sediments including tidal flat deposits (Mosher et al., 2007). Clinoforms preserved on the marginal plateau have thus probably been formed in a shallow marine environment, where the effects of waves and tidal processes could have been predominant. Clinoforms are limited on their upper part by reflection C4 and then covered by homogeneous sedimentation until the top of unit C (Fig 7C). This pattern suggests increasing water depths and probably a forced regression at the end of the clinoform deposition. This observation fits with drill data: C4 corresponds to the base of the Cenomanian-early Campanian black shales. Black shale deposits indicate eutrophic and anoxic environments and were formed during Oceanic Anoxic Events (OAEs, Schlanger and Jenkyns, 1976) that highlight an increase in water depth.

Drill data also reveal that nanofossil chalks then deposited, forming reflection C2. This sedimentary evolution reveals a transition towards a deep, well-oxygenated and more oligotrophic environment (Friedrich and Erbacher, 2006). These observations have been linked by Friedrich and Erbacher (2006) to the opening of the Equatorial Atlantic Gateway (EAG), which was driven by the separation of South America and Africa and led to the connection of the Central and South Atlantic Ocean basins (Förster, 1978). The opening of this gateway, associated with the subsidence of the Rio Grande Rise between ca. 79 and 75 Ma (Murphy and Thomas, 2013), allowed cool South Atlantic intermediate water to invade the proto North Atlantic (Donnadieu et al., 2016; Friedrich et al., 2012) and is thought to have initiated the onset of convection in the Southern Ocean with the formation of the Southern Component Water (SCW) that circulated northward into the Atlantic (Martin et al., 2012;

Murphy and Thomas, 2013; Robinson et al., 2010). The presence of an organic-rich glauconitic interval during this period of major reorganization of deep-water circulation tends to confirm increased ventilation. Despite these observations based on sedimentological data, the seismic data of the upper Cretaceous sedimentary sequence does not display any features (e.g. contourite deposits or bottom-current related features) associated with the onset of deep ocean circulation. This is possibly explained by (1) the presence of a large destabilized complex area (including MTD 01 and MTD 02, e.g. Figs. 7 and 8) that affects down to upper Cretaceous sediment deposits and prevents any clear observation of intermediate or deep bottom-current activities at the scale of the Demerara Plateau during that time, or by (2) the absence, during the Albian, Cenomanian and Turonian, of a fully established large-scale overturning circulation for the South Atlantic, as described by Uenzelmann-Neben et al. (2016).

On the Demerara Plateau, the upper Cretaceous sediments are bounded by an erosive surface (reflection R3, Fig. 4). The isodepth map of this surface shows the same general shape as the isodepth map of reflection R4 (Fig. 5C, zone 1). Reflection R3 corresponds to an erosional surface that correlates with the Cretaceous/Tertiary boundary. In the Demerara ODP drills, this transition is marked by a 2 cm thick bed of impact clay spherules and by a strong drop in benthic foraminiferal abundance, interpreted as a primary air-fall deposit of impact ejecta associated with the Chicxulub meteoroid impact (MacLeod et al., 2007). This major event occurred at a paleodistance of ca. 4500 km (MacLeod et al., 2007). The erosive surface R3 may express a resuspension of sediments on the seafloor shortly after the impact.

Unit B records Paleogene sedimentary conditions on the Demerara Plateau. Isopach maps of sub-unit B2 (Paleocene) and B1 (Eocene/Oligocene) show that sediments infill inherited topographies (Fig. 5D and 5F, zone 1 in particular). The R2 erosional unconformity limits sub-units B2 and B1.

The formation of the R2 erosional unconformity that bounds Paleocene deposits is thought to record the Paleocene-Eocene Thermal Maximum (PETM), one of the most abrupt and significant global warming events (Thomas et al., 2003; Thomas et al., 2002; Zachos et al., 2005). Reflection R2 represents a sedimentary hiatus along the Demerara Plateau (Gouyet, 1988). Bottom-current processes may explain the formation of the R2 erosional surface but the overturning circulation in the South Atlantic is still considered to be weak during Paleocene-Eocene times (Uenzelmann-Neben et al., 2016). On the Demerara Plateau, it is known that bacterial methanogenesis was active during Cenomanian times and that methane has been trapped under Paleocene deposits (O'Regan and Moran, 2007). The

dissolution/dissociation of the gas hydrates may trigger the liquefaction and removal of a large amount of sediments and could explain the origin of the R2 erosional surface. Such observations have already been made along the North West Shelf of Australia by Imbert and Ho (2012).

Eocene-Oligocene deposits (seismic unit B1) overly the R2 unconformity. This period marked the beginning of Cenozoic icehouse conditions (Séranne, 1999) and the Eocene/Oligocene transition coincides with the onset of vigorous circulation in the Atlantic (Katz et al., 2011; Uenzelmann-Neben et al., 2016). The opening of the Drake Passage and climate change are suggested as the cause for this change in circulation. On the Demerara Plateau, no clear influence of thermohaline circulation is observed within the architecture of seismic unit B2 (no erosional surface, no contourite buildups). This is possibly due to the fact that this unit can only be observed on the upper plateau, since a destabilized complex area is present on the intermediate plateau preventing observations further seaward (Fig. 5F).

To summarize, the first stage of evolution and sedimentary infill of the Demerara Plateau since the end of the transform activity is strongly controlled by the thermal subsidence and structure of the margin. The structure and morphology of the plateau influence the distribution pattern of post-transform deposits that tend to infill related depressions. Despite the first modifications in oceanic circulation in the Atlantic during this stage, no clear evidence of current-related erosional surfaces or deposits (contourite drifts) can be observed along the Demerara Plateau. This possibly results from (1) the presence of several MTDs that removed upper Cretaceous and early Cenozoic sediments on the intermediate plateau, or from (2) a still weak global circulation at that time (as suggested by Uenzelmann-Neben et al., 2016) that did not affect sedimentary distributions along the Demerara Plateau.

5.1.2. Transitional stage: middle Miocene to early Pliocene deposits

The transition between the pre-contourite stage and the active contourite stage on the Demerara Plateau is marked by the presence of a major gravitational event (i.e. LM/EP MTD) that erodes sediments down to Paleocene strata (Fig. 6). This MTD rests on reflection R1 on the upper plateau and erodes sedimentary series down to reflection R3 along the intermediate plateau (Fig. 6). Reflection R1 is lower Miocene in age (Ingram et al., 2011). The erosional surface R1 was also identified on the industrial well G2 and described as a sedimentary hiatus

(Gouyet, 1988). The LM/EP MTD could not be strictly dated. Its age can only be assessed relatively to the underlying and overlying strata.

The R1 erosional surface and removal of strata along the Demerara Plateau occurs during a period of major changes in oceanic circulation throughout the Atlantic that led to the permanent establishment of modern thermohaline circulation and the strengthening of the Atlantic Meridional Oceanic Circulation (e.g. Hernández-Molina et al., 2009; Herold et al., 2012; Niemi et al., 2000; Pfuhl and McCave, 2005; Uenzelmann-Neben et al., 2016). The first main paleoceanographic change occurred during the middle Miocene with more vigorous intermediate and deep-water circulation that resulted from the extension of the NADW circulation into the Southern Hemisphere (Kennett, 1982) and the deepening of the AABW circulation (Hernández-Molina et al., 2010; Hernández-Molina et al., 2009; Hernández-Molina et al., 2016; Preu et al., 2013; Preu et al., 2012). At that time, the Central American Seaway was in a deeper position than the level of the NADW outflow (Nisancioglu et al., 2003). Thus, a significant amount of the NADW outflow passed through the Central American Seaway into the Pacific Ocean, reducing the potential amount of NADW outflow transported into the South Atlantic Ocean. Another paleoceanographic change occurred during late Miocene and early Pliocene times and is characterized by a relatively strong activity of the intermediate and deep water circulations. As the Central American Seaway shoaled from ca. 16 to 6 Ma (Haug and Tiedemann, 1998; Nisancioglu et al., 2003), the NADW outflow transported into the Pacific Ocean was strongly reduced. As a result, the NADW circulation increased into the South Atlantic Ocean leading to a more vigorous water circulation pattern at that time (Nisancioglu et al., 2003). Widespread hiatuses and discontinuities in the world's oceans have been observed all over the Atlantic Ocean, both in the Northern and Southern hemispheres, during the middle Miocene, highlighting the importance of the paleoceanographic changes described previously (e.g. Campbell and Mosher, 2016; Miller and Tucholke, 1983). Therefore, the R1 unconformity is coeval with these global paleoceanographic changes and is interpreted as a current-controlled erosion that marks the onset of a deep-water circulation into the Atlantic. Current intensification induced widespread erosion of the underlying topography (Ingram et al., 2011; O'Regan and Moran, 2007) and led to the formation of a peneplain on the Demerara Plateau (Fig. 10A). From that time, the upper Cretaceous and Paleogene sediment deposition patterns were no longer directly influenced by the deep structure of the margin (Figs. 6 and 10A). A similar observation has been made, for instance, in the Arabian Sea, with intensified bottom-current

624 driven erosion leading to the peneplenation of the Sawqirah anticline and the formation of a
625 contourite depositional system (Rodriguez et al., 2016).
626

627 ### 5.1.3. Contourite stage: middle Pliocene to Holocene deposits

628

629 The third stage of evolution of the Demerara Plateau is characterized by the dominant
630 influence of vigorous bottom currents. Indeed, seismic unit A shows an alongslope
631 distribution pattern rather than downslope thinning: layers progressively thin from the upper
632 to the intermediate plateau, disappear where the LM-EP MTD outcrops, and reappear locally,
633 forming thick sedimentary depocenters near the lower plateau (Fig. 10C). In map view, these
634 depocenters are parallel to the edge of the plateau (Fig. 10C) and are interpreted as successive
635 contourite drifts. The onset of this contourite depositional system matches with a lithological
636 change from nannofossil ooze and chalks to overlying clay-rich sediments (Erbacher et al.,
637 2004; Gouyet, 1988; Mosher et al., 2007), as a probable result of the onset of the Amazon
638 River and its transports of fine-grained sediments oceanward. The buildup of the contourite
639 depositional system along the Demerara Plateau follows the establishment of a deep-water
640 circulation in the Atlantic Ocean as described previously. Seismic unit A thus develops as a
641 large depositional feature that we interpret as a plastered drift following the identification
642 criteria based on the literature (e.g. Faugères et al., 1999; Rebesco et al., 2014). At the
643 upper/intermediate plateau transition (i.e. near the main Miocene slope failure headscarp), the
644 proximal part of this plastered drift corresponds to a zone depleted in sediments and
645 interpreted as a channel or an alongslope area with erosional/non-depositional processes
646 (Faugères and Mulder, 2011; Faugères et al., 1999; Rebesco and Stow, 2001). At present, the
647 plastered drift is mainly under the influence of the NADW that flows southeastwardly and the
648 Demerara Plateau could be associated with a contourite terrace that is spatially and vertically
649 affected by the top of the NADW and its transition with the AAIW, as observed on other
650 studies area (e.g. Hernández-Molina et al., 2009; Preu et al., 2013; Rebesco et al., 2014). On
651 the Demerara Plateau, the NADW circulation seems to be guided by the main Miocene slope
652 failure headscarp (Loncke et al., 2016).
653

654 In the distal part of the Demerara Plateau, below 3600 m of water depth, another depleted
655 sediment zone is observed (Fig. 10C, zone 4). It could result from an increased current

velocity near the slope break that marks the transition between the intermediate and lower plateau. It could also be the result of very reduced sedimentation on the distal part of the lower plateau that could thus be considered as sediment starved at present. Interestingly, this area could correspond with the depth range to the interface between the NADW and the AABW. Dominant erosional processes have been reported near this interface in other study areas such as the Argentine and Uruguayan margins (Hernández-Molina et al., 2010; Hernández-Molina et al., 2009; Hernández-Molina et al., 2016; Preu et al., 2013; Preu et al., 2012).

Within plastered drift unit A, sedimentary bedforms that look like sedimentary waves are frequently observed (near the central area of the intermediate plateau). Such sedimentary bedforms are commonly observed within contourite deposits (e.g. Howe, 1996; Rodriguez et al., 2016) and are the results of a secondary circulation, which in many cases are due to the interaction of internal waves with the seafloor (Rebesco et al., 2014). On the Demerara Plateau, sedimentary bedforms appear to be elongated parallel to the main flow direction (i.e. NADW; see Tallobre et al., 2016 for further information). It is thus thought that the formation of these sedimentary bedforms could be related to internal waves.

Within the same timeframe, giant sub-circular depressions forming the Uc unconformity are observed on the upper plateau. Different hypotheses have been made by Pattier et al. (2015) to explain the onset and evolution of these depressions, such as the influence of bottom currents or the presence of pockmarks associated with gas hydrate dissolution (see Pattier et al., 2015 for more details). Similar morphologies have been described in the Gulf of Cadiz (Hernández-Molina et al., 2006; Garcia et al., 2015) and in the South China Sea (Chen et al., 2014; Sun et al., 2017). In the Gulf of Cadiz, a series of crescent-shaped depressions have been identified within the sediment drift. These depressions have been interpreted by Garcia et al. (2015) as the result of complex contourite deposition infilling irregular slide scars due to the local influence of vertical eddies. In the South China Sea, circular to sub-circular depressions have also been observed within a sediment drift. These cut-and-fill erosional features are thought to be caused by the presence of strong vertical eddies and unsteady bottom currents resulting from uneven seabed morphologies (Sun et al., 2017).

On the intermediate plateau, the presence of small-scale to medium-scale mass-transport deposits (MTDS 04, 05, and 06 Fig. 9) located near the Miocene slope failure headscarp indicates that this main slope failure has been maintained active during middle

Pliocene-Holocene times (as testified by the truncation of reflections A7 to A4) probably thanks to bottom-current processes associated with the activity of the NADW.

5.2. Transform marginal plateaus and large-scale hydrodynamic implications

Contourites are sedimentological archives of particular interest since they provide, over a wide range of time scales, information on paleoceanographic conditions (including ocean circulation patterns, current velocities, etc.) linked especially to long-term tectonic plate evolution and climate changes (Rebesco et al., 2014).

Transform marginal plateaus, including the Demerara Plateau, are the place of important contourite systems recording along-slope contour currents (e.g. Hernández-Molina et al., 2010; Jones and Okada, 2006; Laberg et al., 2005; Loncke et al., 2016; Tallobre et al., 2016; Uenzelmann-Neben and Huhn, 2009; Westall et al., 1993). Loncke et al. (2016; submitted) and Tallobre et al. (2016) hypothesize that the presence of marginal plateaus, which extend the continental shelf seaward, may be particularly well suited to enable contourite depositional system development by affecting current dynamics in constraining and accelerating deep current flows. Marginal plateaus could be thus considered as a key target to investigate and better constrain, in the future, the formation and evolution of bottom-current processes. Furthermore, marginal plateaus are located far from continental sediment sources, restricting the formation of turbidites that are related to high-density turbidity currents (Lowe, 1982), as observed on the Demerara Plateau. The interaction between downslope density currents and alongslope contour currents is often observed when both processes take place along the same margin (Brackenridge et al., 2011; Hernández-Molina et al., 2006; Marchès et al., 2010; Rebesco et al., 2002), and lead to the formation of mixed turbidite/contourite depositional systems (Rebesco et al., 2014). It can be rather difficult to identify and differentiate sedimentary bodies that are related to turbidity or contour currents. Since transform marginal plateaus are located far from continental sedimentary sources, the contourites they host are probably less perturbed by turbidites.

Finally, since transform marginal plateaus represent the last contact point during continental breakup and subsequent oceanization, they may be particularly sensitive to the onset and changes of oceanographic conditions through time (Loncke et al., submitted). However, in the case of the Demerara Plateau, numerous mass transport deposits, possibly related to

contourite processes, prevent us from documenting the possible pre-Miocene initial stages of the Atlantic bottom water circulation.

6. Conclusion

Our synthetic analysis provides a refined image of the post-transform architecture of the outer Demerara marginal plateau and a better understanding of the intricate relations between topography, bottom currents activity and slope instabilities that influence sedimentation on the plateau.

From the late Albian to the early Miocene (Pre-contourite Stage), the evolution and sedimentary infill of the Demerara Plateau are strongly controlled by structural topographic inheritances. The difference of structure and morphology between the transform and divergent segments directly influences through a differential subsidence the distribution pattern of post-transform deposits. Despite the first modifications in oceanic circulation in the Atlantic during this stage, no clear evidence of a large-scale overturning circulation has been observed along the Demerara Plateau, possibly erased by the regular mechanical destabilization of the plateau that occurs since the upper Cretaceous.

The transition between the pre-contourite stage and the active contourite stage (Transitional Stage, middle Miocene to early Pliocene) is associated with a major gravitational event that erodes sediments down to Paleocene strata. The basal décollement layer of this mass transport deposit corresponds to an erosive event that peneplains the distal plateau and is middle Miocene in age. It is interpreted as the result of major changes in oceanic circulation throughout the Atlantic linked notably to the progressive closure of the Central American Seaway that has induced the onset of a modern and intensified in strength Atlantic Meridional Oceanic Circulation.

The establishment of a persistent deep-water circulation into the Atlantic leads to the development of current-controlled sedimentary features during middle Pliocene-Holocene times. Depositional (e.g. plastered drift, sedimentary bedforms) and erosional (e.g. channels, furrows) features developed thus under the influence of NADW and AAIW as well as the interface between the two water masses. These contourite features enable us to identify a contourite depositional system along the Demerara Plateau. The NADW seems to be guided by the main Miocene slope failure headscarp that localizes a zone depleted in sediments and interpreted as a channel or an alongslope area with erosional/non-depositional processes.

Bottom-current processes associated with the activity of the NADW maintained the main Miocene slope failure headscarp active during middle Pliocene-Holocene times. MTDs are thus commonly observed within the plastered drift. Outcropping MTDs directly influence the distribution pattern of contourite deposits and alter locally the hydrodynamic regime allowing the formation of sedimentary bedforms along the plastered drift. It results a complex interaction between downslope and alongslope processes on the Demerara Plateau.

In constraining and accelerating deep current flows, marginal plateaus are particularly prone to develop contourite depositional system. Marginal plateaus should be considered as a key target to investigate and better constraint the formation and evolution of bottom current processes.

Acknowledgements

We thank IFREMER for the funding of F. Pattier's Ph.D. and TOTAL SA, which made available shallow parts of the industrial seismic dataset for interpretation in the context of this Ph.D. We also deeply thank the scientific IGUANES party for processing the seismic dataset used in this paper. We also thank the MARGATS and DRADEM head scientists (D. Graindorge, W. Roest, F. Klingelhoefer, C. Basile) for access to the bathymetric data acquired during their campaigns. Part of this research was conducted within the framework of "The Drifters Research Group" of the Royal Holloway University of London (UK) and is related to projects CTM2012-39599-C03, CGL2016-80445-R, and CTM2016-75129-C3-1-R. Finally, we deeply thank two anonymous reviewers and the editor for their very useful comments and suggestions that helped to improve the manuscript.

References

Alvarez, L.W., Alvarez, W., Asaro, F., Michel, H.V., 1980. Extraterrestrial Cause for the Cretaceous-Tertiary Extinction. Science 208, 1095-1108.

Bartoli, G., Sarnthein, M., Weinelt, M., Erlenkeuser, H., Garbe-Schönberg, D., Lea, D.W., 2005. Final closure of Panama and the onset of northern hemisphere glaciation. Earth and Planetary Science Letters 237, 33-44.

Basile, C., 2015. Transform continental margins — part 1: Concepts and models. Tectonophysics 661, 1-10.

Basile, C., Maillard, A., Patriat, M., Gaullier, V., Loncke, L., Roest, W., Mercier de Lépinay, M., Pattier, F., 2013. Structure and evolution of the Demerara Plateau, offshore French Guiana: Rifting, tectonic inversion and post-rift tilting at transform–divergent margins intersection. Tectonophysics 591, 16-29.

Benkhelil, J., Mascle, J., Tricart, P., 1995. The Guinea continental margin: an example of a structurally complex transform margin. Tectonophysics 248, 117-137.
Brackenridge, R., Stow, D.A.V., Hernández-Molina, F.J., 2011. Contourites within a deep-water sequence stratigraphic framework. Geo-Marine Letters 31, 343-360.
Bryn, P., Berg, K., Forsberg, C.F., Solheim, A., Kvalstad, T.J., 2005. Explaining the Storegga Slide. Marine and Petroleum Geology 22, 11-19.
Campan, A., 1995. Analyse cinématique de l'Atlantique équatorial : implcations sur l'évolution de l'Atlantique Sud et sur la frontière de plaques Amérique du Nord/Amérique du Sud. Université Pierre et Marie Curie, p. 352.
Campbell, D.C., Mosher, D.C., 2016. Geophysical evidence for widespread Cenozoic bottom current activity from the continental margin of Nova Scotia, Canada. Marine Geology 378, 237-260.
Cattaneo, A., Trincardi, F., Asioli, A., Correggiari, A., 2007. The Western Adriatic shelf clinoform: energy-limited bottomset. Continental Shelf Research 27, 506-525.
Dailly, P., Henderson, T., Hudgens, E., Kanschat, K., Lowry, P., 2013. Exploration for Cretaceous stratigraphic traps in the Gulf of Guinea, West Africa and the discovery of the Jubilee Field: a play opening discovery in the Tano Basin, Offshore Ghana. Geological Society, London, Special Publications 369, 235-248.
Donnadieu, Y., Pucéat, E., Moiroud, M., Guillocheau, F., Deconinck, J.-F., 2016. A better-ventilated ocean triggered by Late Cretaceous changes in continental configuration. 7, 10316.
Emery, D., Myers, K.J., 1996. Sequence stratigraphy. Blackwell Science, Oxford.
Erbacher, J., Mosher, D.C., Malone, M.J., et al., 2004. Proceedings of the Ocean Drilling Program, Initial Reports 207: College Station, TX (Ocean Drilling Program).
Fail, J.P., Montadert, L., Delteil, J.R., Valery, P., Patriat, P., Schlich, R., 1970. Prolongation des zones de fractures de l'ocean atlantique dans le golfe de guinee. Earth and Planetary Science Letters 7, 413-419.
Faugères, J.-C., Gonthier, E., Stow, D.A.V., 1984. Contourite drift molded by deep Mediterranean outflow. Geology 12, 296-300.
Faugères, J.-C., Stow, D.A.V., Imbert, P., Viana, A., 1999. Seismic features diagnostic of contourite drifts. Marine Geology 162, 1-38.
Förster, R., 1978. Evidence for an open seaway between northern and southern proto-Atlantic in Albian times. Nature 272, 158-159.
Friedrich, O., Erbacher, J., 2006. Benthic foraminiferal assemblages from Demerara Rise (ODP Leg 207, western tropical Atlantic): possible evidence for a progressive opening of the Equatorial Atlantic Gateway. Cretaceous Research 27, 377-397.
Friedrich, O., Norris, R.D., Erbacher, J., 2012. Evolution of middle to Late Cretaceous oceans—A 55 m.y. record of Earth's temperature and carbon cycle. Geology 40, 107-110.
Gaullier, V., Loncke, L., Droz, L., Basile, C., Maillard, A., Patriat, M., Roest, W.R., Loubrieu, B., Folens, L., Carol, F., 2010. Slope Instability on the French Guiana Transform Margin from Swath-Bathymetry and 3.5 kHz Echograms, in: Mosher, D.C., Shipp, R.C., Moscardelli, L., Chaytor, J.D., Baxter, C.D.P., Lee, H.J., Urgeles, R. (Eds.), Submarine Mass Movements and Their Consequences. Springer Netherlands, Dordrecht, pp. 569-579.
Gouyet, S., 1988. Evolution tectono-sédimentaire des marges guyanaise et nord-brésilienne au cours de l'ouverture de l'Atlantique Sud. University of Pau and Pays de l'Adour, p. 363.
Greenroyd, C.J., Peirce, C., Rodger, M., Watts, A.B., Hobbs, R.W., 2007. Crustal structure of the French Guiana margin, West Equatorial Atlantic. Geophysical Journal International 169, 964-987.
Greenroyd, C.J., Peirce, C., Rodger, M., Watts, A.B., Hobbs, R.W., 2008. Demerara Plateau — the structure and evolution of a transform passive margin. Geophysical Journal International 172, 549-564.
Hardage, B.A., 1987. Seismic stratigraphy. Geophysocal Press, University of California.
Haug, G.H., Tiedemann, R., 1998. Effect of the formation of the Isthmus of Panama on Atlantic Ocean thermohaline circulation. Nature 393, 673-676.

Heezen, B.C., Hollister, C., 1964. Deep-sea current evidence from abyssal sediments. Marine Geology 1, 141-174.

Hernández-Molina, F.J., Llave, E., Stow, D.A.V., García, M., Somoza, L., Vázquez, J.T., Lobo, F.J., Maestro, A., Díaz del Río, V., León, R., Medialdea, T., Gardner, J., 2006. The contourite depositional system of the Gulf of Cádiz: A sedimentary model related to the bottom current activity of the Mediterranean outflow water and its interaction with the continental margin. Deep Sea Research Part II: Topical Studies in Oceanography 53, 1420-1463.

Hernández-Molina, F.J., Paterlini, M., Somoza, L., Violante, R., Arecco, M.A., de Isasi, M., Rebesco, M., Uenzelmann-Neben, G., Neben, S., Marshall, P., 2010. Giant mounded drifts in the Argentine Continental Margin: Origins, and global implications for the history of thermohaline circulation. Marine and Petroleum Geology 27, 1508-1530.

Hernández-Molina, F.J., Paterlini, M., Violante, R., Marshall, P., de Isasi, M., Somoza, L., Rebesco, M., 2009. Contourite depositional system on the Argentine Slope: An exceptional record of the influence of Antarctic water masses. Geology 37, 507-510.

Hernández-Molina, F.J., Soto, M., Piola, A.R., Tomasini, J., Preu, B., Thompson, P., Badalini, G., Creaser, A., Violante, R.A., Morales, E., Paterlini, M., De Santa Ana, H., 2016. A contourite depositional system along the Uruguayan continental margin: Sedimentary, oceanographic and paleoceanographic implications. Marine Geology 378, 333-349.

Herold, N., Huber, M., Müller, R.D., Seton, M., 2012. Modeling the Miocene climatic optimum: Ocean circulation. Paleoceanography 27, n/a-n/a.

Howe, J.A., 1996. Turbidite and contourite sediment waves in the northern Rockall Trough, North Atlantic Ocean. Sedimentology 43, 219-234.

IHO, 2008. International Hydrographic Organization (IHO) standards for hydrographic surveys, 5th edition, February 2008. Monaco, International Hydrographic Bureau, 28pp. .

Imbert, P., Ho, S., 2012. Seismic-scale funnel-shaped collapse features from the Paleocene–Eocene of the North West Shelf of Australia. Marine Geology 332–334, 198-221.

Ingram, W.C., Mosher, D.C., Wise, S.W.J., 2011. Biostratigraphy of an Upper Miocene mass transport deposit on Demerara Rise, northern South American Margin, in: Shipp, C., Weimer, P., Posamentier, H. (Eds.), Mass-transport deposits in deepwater settings. SEPM Special Publication, pp. 457-498.

Johns, W.E., Fratantoni, D.M., Zantopp, R.J., 1993. Deep western boundary current variability off northeastern Brazil. Deep Sea Research Part I: Oceanographic Research Papers 40, 293-310.

Jones, E.J.W., Okada, H., 2006. Abyssal circulation change in the equatorial Atlantic: Evidence from Cenozoic sedimentary drifts off West Africa. Marine Geology 232, 49-61.

Katz, M.E., Cramer, B.S., Toggweiler, J.R., Esmay, G., Liu, C., Miller, K.G., Rosenthal, Y., Wade, B.S., Wright, J.D., 2011. Impact of Antarctic Circumpolar Current Development on Late Paleogene Ocean Structure. Science 332, 1076-1079.

Kennett, J., 1982. Marine Geology. Prentice-Hall, University of California.

Kennett, J.P., Cannariato, K.G., Hendy, I.L., Behl, R.J., 2000. Carbon Isotopic Evidence for Methane Hydrate Instability During Quaternary Interstadials. Science 288, 128-133.

Laberg, J.S., Dahlgren, K.I.T., Vorren, T.O., 2005. The Eocene–late Pliocene paleoenvironment in the Vøring Plateau area, Norwegian Sea—paleoceanographic implications. Marine Geology 214, 269-285.

Le Pichon, X., Hayes, D.E., 1971. Marginal offsets, fracture zones, and the early opening of the South Atlantic. Journal of Geophysical Research 76, 6283-6293.

Loncke, L., Droz, L., Gaullier, V., Basile, C., Patriat, M., Roest, W., 2009. Slope instabilities from echo-character mapping along the French Guiana transform margin and Demerara abyssal plain. Marine and Petroleum Geology 26, 711-723.

Loncke, L., Maillard, A., Basile, C., Roest, W.R., Bayon, G., Gaullier, V., Pattier, F., Mercier de Lépinay, M., Grall, C., Droz, L., Marsset, T., Giresse, P., Caprais, J.C., Cathalot, C., Graindorge, D., Heuret, A., Lebrun, J.F., Bermell, S., Marcaillou, B., Sotin, C., Hebert, B., Patriat, M., Bassetti, M.A., Tallobre, C., Buscail, R., Durrieu de Madron, X., Bourrin, F., 2016. Structure of the Demerara passive-transform margin and associated sedimentary processes. Initial results from the IGUANES cruise. Geological Society, London, Special Publications 431, 179-197.

Lowe, D.R., 1982. Sediment gravity flows; II, Depositional models with special reference to the deposits of high-density turbidity currents. Journal of Sedimentary Research 52, 279-297.

MacLeod, K.G., Whitney, D.L., Huber, B.T., Koeberl, C., 2007. Impact and extinction in remarkably complete Cretaceous-Tertiary boundary sections from Demerara Rise, tropical western North Atlantic. GSA Bulletin 119, 101-115.

Marchès, E., Mulder, T., Gonthier, E., Cremer, M., Hanquiez, V., Garlan, T., Lecroart, P., 2010. Perched lobe formation in the Gulf of Cadiz: Interactions between gravity processes and contour currents (Algarve Margin, Southern Portugal). Sedimentary Geology 229, 81-94.

Martin, E.E., MacLeod, K.G., Jiménez Berrocoso, A., Bourbon, E., 2012. Water mass circulation on Demerara Rise during the Late Cretaceous based on Nd isotopes. Earth and Planetary Science Letters 327–328, 111-120.

Mascle, J., 1976. Atlantic-type continental margins - distinction of two basic structural types. An. Acad. Bras. Cienc 48, 191-197.

Mascle, J., Marinho, M., Wannesson, J., 1986. The structure of the guinean continental margin: Implications for the connection between the central and the south atlantic oceans. Geologische Rundschau 75, 57-70.

Mauritzen, C., Polzin, K.L., McCartney, M.S., Millard, R.C., West-Mack, D.E., 2002. Evidence in hydrography and density fine structure for enhanced vertical mixing over the Mid-Atlantic Ridge in the western Atlantic. Journal of Geophysical Research: Oceans 107, 3147-3166.

Mercier de Lépinay, M., Loncke, L., Basile, C., Roest, W.R., Patriat, M., Maillard, A., De Clarens, P., 2016. Transform continental margins – Part 2: A worldwide review. Tectonophysics 693, Part A, 96-115.

Miller, K.G., Tucholke, B.E., 1983. Development of Cenozoic Abyssal Circulation South of the Greenland-Scotland Ridge, in: Bott, M.H.P., Saxov, S., Talwani, M., Thiede, J. (Eds.), Structure and Development of the Greenland-Scotland Ridge: New Methods and Concepts. Springer US, Boston, MA, pp. 549-589.

Morley, C.K., 2015. Cenozoic structural evolution of the Andaman Sea: evolution from an extensional to a sheared margin. Geological Society, London, Special Publications 431, 39-61.

Mosher, D.C., Erbacher, J., Malone, M.J., 2007. Proceedings of the Ocean Drilling Program, Scientic Results 207: College Station, TX (Ocean Drilling Program).

Moulin, M., Aslanian, D., Unternehr, P., 2010. A new starting point for the South and Equatorial Atlantic Ocean. Earth-Science Reviews 98, 1-37.

Murphy, D.P., Thomas, D.J., 2013. The evolution of Late Cretaceous deep-ocean circulation in the Atlantic basins: Neodymium isotope evidence from South Atlantic drill sites for tectonic controls. Geochemistry, Geophysics, Geosystems 14, 5323-5340.

Nemčok, M., Rybár, S., Sinha, S.T., Hermeston, S.A., Ledvényiová, L., 2016. Transform margins: development, controls and petroleum systems – an introduction. Geological Society, London, Special Publications 431, 1-38.

Nielsen, T., Knutz, P.C., Kuijpers, A., 2008. Chapter 16 Seismic Expression of Contourite Depositional Systems, in: Rebesco, M., Camerlenghi, A. (Eds.), Developments in Sedimentology. Elsevier, pp. 301-321.

Niemi, T.M., Ben-Avraham, Z., Hartnady, C.J.H., Reznikov, M., 2000. Post-Eocene seismic stratigraphy of the deep ocean basin adjacent to the southeast African continental margin: a record of geostrophic bottom current systems. Marine Geology 162, 237-258.

Nisancioglu, K.H., Raymo, M.E., Stone, P.H., 2003. Reorganization of Miocene deep water circulation in response to the shoaling of the Central American Seaway. Paleoceanography 18.

O'Regan, M., Moran, K., 2007. Compressibility, permeability and stress history of sediments from Demerara Rise, in: Mosher, D.C., Erbacher, J., Malone, M.J. (Eds.), Proceedings of the Ocean Drilling Program, Scientific Results 2007. Ocean Drilling Program, College Station, TX.

Patruno, S., Hampson, G.J., Jackson, C.A.L., 2015. Quantitative characterisation of deltaic and subaqueous clinoforms. Earth-Science Reviews 142, 79-119.

Pattier, F., Loncke, L., Gaullier, V., Basile, C., Maillard, A., Imbert, P., Roest, W.R., Vendeville, B.C., Patriat, M., Loubrieu, B., 2013. Mass-transport deposits and fluid venting in a transform margin setting, the eastern Demerara Plateau (French Guiana). Marine and Petroleum Geology 46, 287-303.

Pattier, F., Loncke, L., Imbert, P., Gaullier, V., Basile, C., Maillard, A., Roest, W.R., Patriat, M., Vendeville, B.C., Marsset, T., Bayon, G., Cathalot, C., Caprais, J.C., Bermell, S., Sotin, C., Hebert, B., Mercier de Lépinay, M., Lebrun, J.F., Marcaillou, B., Heuret, A., Droz, L., Graindorge, D., Poetisi, E., Berrenstein, H., 2015. Origin of an enigmatic regional Mio-Pliocene unconformity on the Demerara plateau. Marine Geology 365, 21-35.

Payton, C.E., 1977. Seismic Stratigraphy — Applications to Hydrocarbon Exploration, Tulsa, Oklahoma.

Peterson, R.G., Stramma, L., 1991. Upper-level circulation in the South Atlantic Ocean. Progress in Oceanography 26, 1-73.

Pfuhl, H.A., McCave, I.N., 2005. Evidence for late Oligocene establishment of the Antarctic Circumpolar Current. Earth and Planetary Science Letters 235, 715-728.

Preu, B., Hernández-Molina, F.J., Violante, R., Piola, A.R., Paterlini, C.M., Schwenk, T., Voigt, I., Krastel, S., Spiess, V., 2013. Morphosedimentary and hydrographic features of the northern Argentine margin: The interplay between erosive, depositional and gravitational processes and its conceptual implications. Deep Sea Research Part I: Oceanographic Research Papers 75, 157-174.

Preu, B., Schwenk, T., Hernández-Molina, F.J., Violante, R., Paterlini, M., Krastel, S., Tomasini, J., Spieß, V., 2012. Sedimentary growth pattern on the northern Argentine slope: The impact of North Atlantic Deep Water on southern hemisphere slope architecture. Marine Geology 329-331, 113-125.

Rebesco, M., 2005. Contourites, in: Selley, R.C., Cocks, L.R.M., Plimer, I.R. (Eds.), Encyclopedia of Geology. Elsevier, London, pp. 513-527.

Rebesco, M., Camerlenghi, A., 2008. Contourites. Elsevier, Amsterdam.

Rebesco, M., Hernández-Molina, F.J., Van Rooij, D., Wåhlin, A., 2014. Contourites and associated sediments controlled by deep-water circulation processes: State-of-the-art and future considerations. Marine Geology 352, 111-154.

Rebesco, M., Pudsey, C.J., Canals, M., Camerlenghi, A., Barker, P.F., Estrada, F., Giorgetti, A., 2002. Sediment drifts and deep-sea channel systems, Antarctic Peninsula Pacific Margin. Geological Society, London, Memoirs 22, 353-371.

Reuber, K.R., Pindell, J., Horn, B.W., 2016. Demerara Rise, offshore Suriname: Magma-rich segment of the Central Atlantic Ocean, and conjugate to the Bahamas hot spot. Interpretation 4, T141-T155.

Robinson, S.A., Murphy, D.P., Vance, D., Thomas, D.J., 2010. Formation of “Southern Component Water” in the Late Cretaceous: Evidence from Nd-isotopes. Geology 38, 871-874.

Rodriguez, M., Bourget, J., Chamot-Rooke, N., Huchon, P., Fournier, M., Delescluse, M., Zaragosi, S., 2016. The Sawqirah contourite drift system in the Arabian Sea (NW Indian Ocean): A case study of interactions between margin reactivation and contouritic processes. Marine Geology 381, 1-16.

Sapin, F., Davaux, M., Dall'Asta, M., Lahmi, M., Baudot, G., Ringenbach, J.-C., 2016. Post-rift subsidence of the French Guiana hyper-oblique margin: from rift-inherited subsidence to Amazon deposition effect. Geological Society, London, Special Publications 431, 125-144.

Schlanger, S.O., Jenkyns, H.C., 1976. Cretaceous Oceanic Anoxic Events: causes and consequences. Geologie en Mijnbouw 55, 179-184.

Schlitzer, R., 2017. Ocean Data View, odv.awi.de, 2017.

Séranne, M., 1999. Early Oligocene stratigraphic turnover on the west Africa continental margin: a signature of the Tertiary greenhouse-to-icehouse transition? Terra Nova 11, 135-140.

Sondag, F., Guyot, J.L., Moquet, J.S., Laraque, A., Adele, G., Cochonneau, G., Doudou, J.C., Lagane, C., Vauchel, P., 2010. Suspended sediment and dissolved load budgets of two Amazonian rivers from the Guiana Shield: Maroni River at Langa Tabiki and Oyapock River at Saut Maripa (French Guiana). Hydrological Processes 24, 1433-1445.

Stow, D.A.V., Faugères, J.-C., Howe, J.A., Pudsey, C.J., Viana, A.R., 2002. Bottom currents, contourites and deep-sea sediment drifts: current state-of-the-art. Geological Society, London, Memoirs 22, 7-20.

998 Stow, D.A.V., Faugères, J.C., 2008. Chapter 13 Contourite Facies and the Facies Model, in: Rebesco,
999 M., Camerlenghi, A. (Eds.), Developments in Sedimentology. Elsevier, pp. 223-256.
1000 Suga, T., Talley, L.D., 1995. Antarctic Intermediate Water circulation in the tropical and subtropical
1001 South Atlantic. Journal of Geophysical Research: Oceans 100, 13441-13453.
1002 Tallobre, C., Loncke, L., Bassetti, M.-A., Giresse, P., Bayon, G., Buscail, R., de Madron, X.D., Bourrin, F.,
1003 Vanhaesebroucke, M., Sotin, C., 2016. Description of a contourite depositional system on the
1004 Demerara Plateau: Results from geophysical data and sediment cores. Marine Geology 378, 56-73.
1005 Thomas, D.J., Bralower, T.J., Jones, C.E., 2003. Neodymium isotopic reconstruction of late Paleocene–
1006 early Eocene thermohaline circulation. Earth and Planetary Science Letters 209, 309-322.
1007 Thomas, D.J., Zachos, J.C., Bralower, T.J., Thomas, E., Bohaty, S., 2002. Warming the fuel for the fire:
1008 Evidence for the thermal dissociation of methane hydrate during the Paleocene-Eocene thermal
1009 maximum. Geology 30, 1067-1070.
1010 Tourtelot, H.A., 1979. Black shale - its deposition and diagenesis. Clays and Clay Minerals 27, 313-
1011 321.
1012 Tsuchiya, M., Talley, L.D., McCartney, M.S., 1994. Water-mass distributions in the western South
1013 Atlantic; a section from South Georgia Island (54S) northward across the equator. Journal of Marine
1014 Research 52, 55-81.
1015 Uenzelmann-Neben, G., Huhn, K., 2009. Sedimentary deposits on the southern South African
1016 continental margin: Slumping versus non-deposition or erosion by oceanic currents? Marine Geology
1017 266, 65-79.
1018 Uenzelmann-Neben, G., Weber, T., Grützner, J., Thomas, M., 2016. Transition from the Cretaceous
1019 ocean to Cenozoic circulation in the western South Atlantic — A twofold reconstruction.
1020 Tectonophysics, http://dx.doi.org/10.1016/j.tecto.2016.1005.1036.
1021 Unternehr, P., Curie, D., Olivet, J.L., Goslin, J., Beuzart, P., 1988. South Atlantic fits and intraplate
1022 boundaries in Africa and South America. Tectonophysics 155, 169-179.
1023 Westall, F., Rossi, S., Mascle, J., 1993. Current-controlled sedimentation in the Equatorial Atlantic:
1024 examples from the southern margin of the Guinea Plateau and the Romanche Fracture Zone.
1025 Sedimentary Geology 82, 157-171.
1026 Wilson, J.T., 1965. A New Class of Faults and their Bearing on Continental Drift. Nature 207, 343-347.
1027 Yamada, Y., Kawamura, K.I., Ogawa, Y., Urgeles, R., Mosher, D., Chaytor, J., Strasser, M., 2012.
1028 Submarine Mass Movements and Their Consequences, Advances in Natural and Technological
1029 Hazards Research. Springer Science.
1030 Zachos, J.C., Röhl, U., Schellenberg, S.A., Sluijs, A., Hodell, D.A., Kelly, D.C., Thomas, E., Nicolo, M.,
1031 Raffi, I., Lourens, L.J., McCarren, H., Kroon, D., 2005. Rapid Acidification of the Ocean During the
1032 Paleocene-Eocene Thermal Maximum. Science 308, 1611-1615.

1033

1034

1035

Figure captions

Figure 1: (A) Map of South America illustrating the position of the studied area (Demerara Plateau) and the general circulation of the main deep-water masses (based on Brackenbridge et al., 2011). The position of the two main ocean gateways (i.e. Drake Passage and Central American Seaway (CAS)) in the South Atlantic is also reported. NADW: North Atlantic Deep Water; AABW: Antarctic Bottom Water. (B) Location of the Demerara marginal plateau off French Guiana and Surinam, showing the main rivers surrounding the studied area (i.e. the Amazon, Orinoco, Maroni and Oyapock Rivers) and their watershed. Black arrows indicate the transform segment of the margin. (C) Detailed bathymetric map of the Demerara marginal plateau, including the HOMONIM (SHOM) digital elevation model that allows the representation of the Amazon-Guianas mobile mud belt. Location of the seismic lines presented in Figs. 6, 7, 8 and 9 are shown in addition to well drilling of ODP Leg 207 (Mosher et al., 2007) and well G2 (Gouyet, 1988).

Figure 2: Detailed bathymetric map illustrating the four main physiographic domains of the Demerara Plateau (i.e. the upper plateau, the intermediate plateau, the lower plateau and the abyssal plain). Note the presence of the main NW-SE Miocene slope failure headscarp that forms an abrupt incision on the bathymetry and marks the transition between the upper and intermediate plateau (Fig. 2A). Seafloor depressions are also illustrated by close-up views (Figs. 2A and 2B).

Figure 3: (A) Location of the A20 hydrographic section (stations 71 to 95; Koltermann et al., 2011) illustrating the distribution of the water masses on the Demerara Plateau. (B) Potential temperature vs. salinity plot allowing the identification of water-mass structures on the Demerara Plateau. (B) Distribution of the water masses (identified on Fig. 3B) and (D) salinity profile of water masses along the Demerara Plateau. c.s.: continental slope; u.p.: upper plateau; i.p.: intermediate plateau; l.p.: lower plateau; c.sl.: continental slope; a.p.: abyssal plain.

Figure 4: Regional stratigraphy of post-transform discontinuities and seismic units identified along the Demerara Plateau. Chronology of the main mass-transport deposits (MTD1*, MTD2* and LM/EP MTD* are from Pattier et al., 2013, 2015) has also been reported, as well as lithological units known from ODP Leg 207 drillings (Mosher et al., 2007) and the G2 well

(Gouyet, 1988). Note that seismic units C and B are related to the pre-contourite stage, while seismic unit A corresponds to the contourite stage. R1 unconformity and late Miocene/early Pliocene MTD are interpreted as a transitional stage.

Figure 5: Isodepth and isopach maps of the late Albian/middle Miocene pre-contourite discontinuities (i.e. reflections R4 (late Albian), R3 (Cretaceous/Tertiary transition) and R2 (PETM climate event)) and units (i.e. seismic unit C, B2 and B1).

Figure 6: (A) Seismic profile across the entire Demerara marginal plateau and (B) its interpretation.

Figure 7: (A) High-resolution 72-trace seismic profile (location in Fig. 2) illustrating the architecture of post-transform deposits on the Demerara Plateau. The intermediate plateau is characterized by the presence of several MTDs that affect down to upper Cretaceous sediment deposits. (B) Within contourite deposits (seismic unit A, which overlies reflection R1 and the LM/EP MTD), giant depressions are observed on the upper plateau. (C) Preserved clinoforms within seismic unit C on the intermediate plateau.

Figure 8: (A) High-resolution 72-trace seismic profile (location in Fig. 2) illustrating pre-contourite and contourite deposits on the Demerara Plateau. Pre-contourite deposits are affected by a large destabilized complex area observed on the intermediate plateau. Small pockmarks as well as sedimentary ridges developed within the contourite depositional system. (B) Close-up view of the main slope failure headscarp that is expressed on the bathymetry as an abrupt incision. (C) The presence of comet tails is commonly observed when MTDs outcrop on the Demerara Plateau.

Figure 9: (A) High-resolution 72-trace seismic profile (location in Fig. 2) illustrating the relation between alongslope and downslope processes. (B) and (C) correspond to close-up views of the most recent MTDs (i.e. MTDs 05 and 06) observed within contourite deposits (seismic unit A). These small- to medium-scale MTDs are observed immediately downward of the Miocene slope failure headscarp, suggesting that this one is regularly reactivated.

Figure 10: Isodepth and isopach maps of the transitional middle Miocene R1 discontinuity and LM/EP MTD, as well as an isopach map of the middle Pliocene-Holocene contourite depositional system (i.e. seismic unit A).

Highlights

1. The post-transform sedimentation of the Demerara marginal plateau (DP) is studied
2. A strong relation between topography, downslope and alongslope processes shapes DP
3. Marginal plateaus are particularly prone to develop contourite deposits

Declaration of interests

☒ The authors declare that they have no known competing financial interests or personal relationships that could have appeared to influence the work reported in this paper.

☐The authors declare the following financial interests/personal relationships which may be considered as potential competing interests:

Figure 1

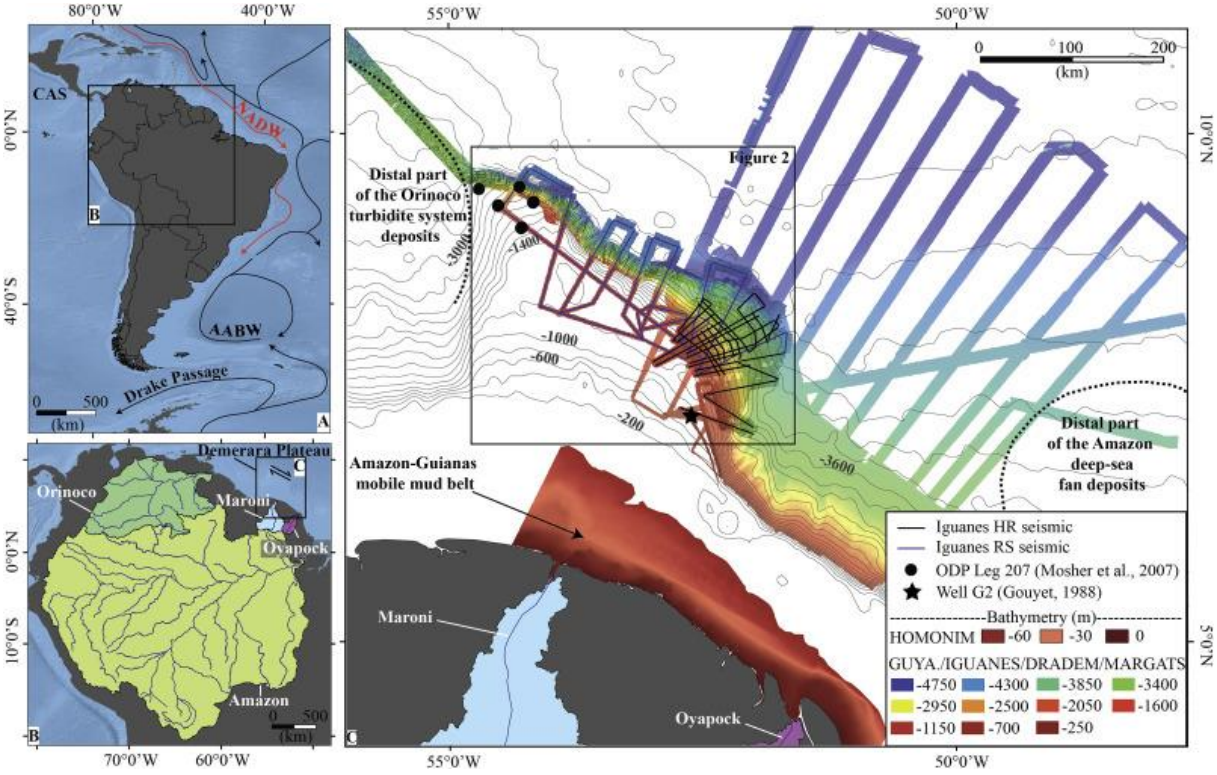
80°0'W
40°0'W
55°0'W
50°0'W
0°0'N
40°0'S
10°0'N
5°0'N
70°0'W
60°0'W
CAS
NADW
AABW
Drake Passage
0 500 (km)
A
B
Demerara Plateau
C
Orinoco
Maroni
Oyapock
Amazon
0 100 200 (km)
Figure 2
Distal part of the Orinoco turbidite system deposits
-3000
-1400
-1000
-600
-200
-3600
Distal part of the Amazon deep-sea fan deposits
Amazon-Guianas mobile mud belt
Iguanes HR seismic
Iguanes RS seismic
ODP Leg 207 (Mosher et al., 2007)
Well G2 (Gouyet, 1988)
Bathymetry (m)
HOMONIM -60 -30 0
GUYA./IGUANES/DRADEM/MARGATS
-4750 -4300 -3850 -3400
-2950 -2500 -2050 -1600
-1150 -700 -250

Figure 2

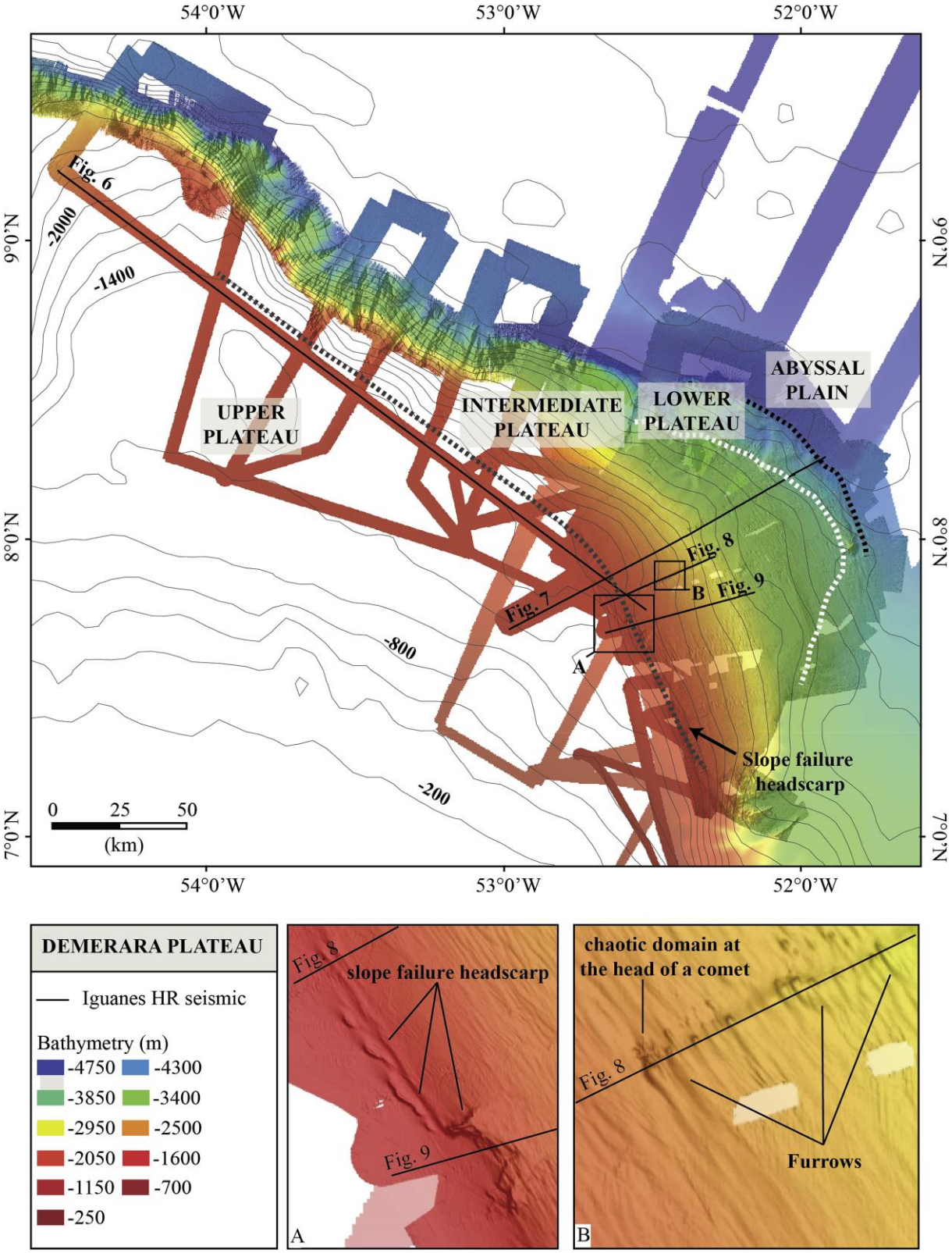
54°0'W
53°0'W
52°0'W
9°0'N
8°0'N
7°0'N
Fig. 6
-2000
-1400
UPPER PLATEAU
INTERMEDIATE PLATEAU
LOWER PLATEAU
ABYSSAL PLAIN
Fig. 8
B Fig. 9
Fig. 7
A
-800
-200
Slope failure headscarp
0 25 50
(km)
DEMERARA PLATEAU
Iguanes HR seismic
Bathymetry (m)
-4750 -4300
-3850 -3400
-2950 -2500
-2050 -1600
-1150 -700
-250
Fig. 8
slope failure headscarp
Fig. 9
A
chaotic domain at the head of a comet
Fig. 8
Furrows
B

Figure 3

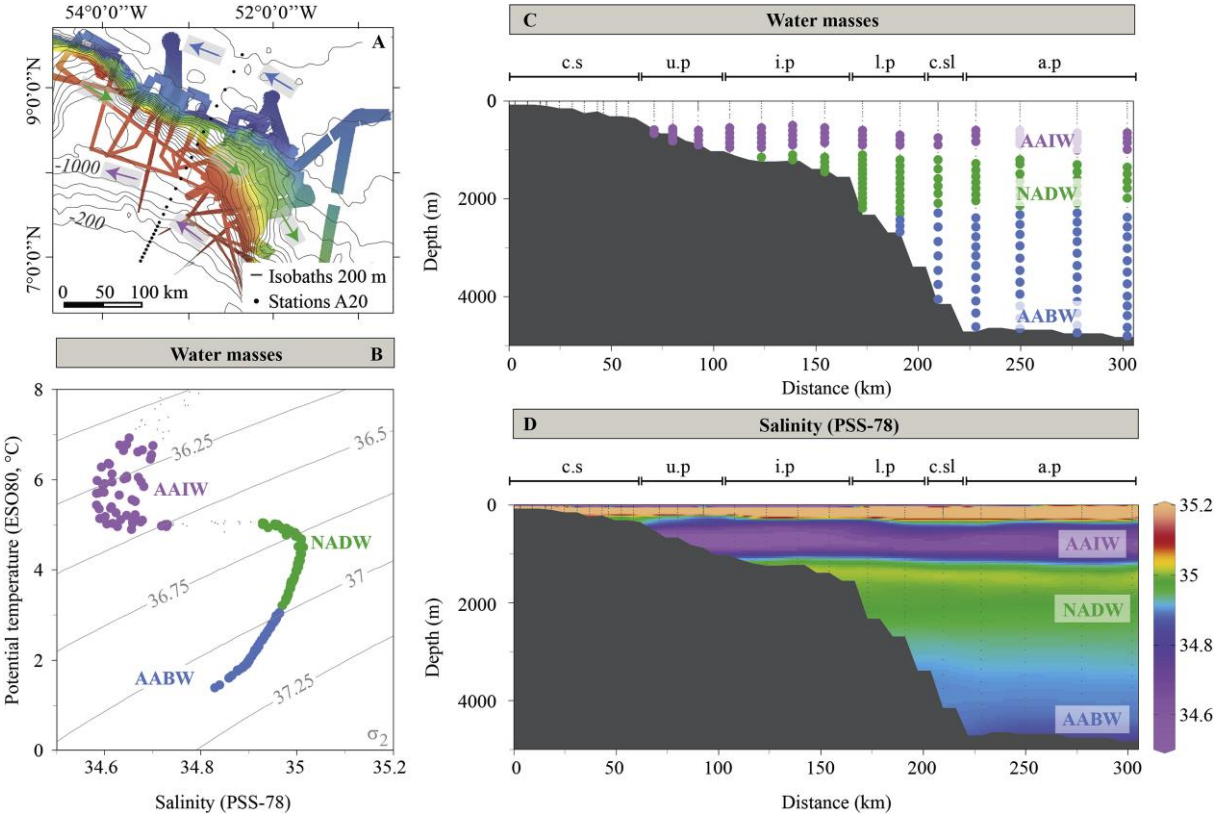
54°0'0"W
52°0'0"W
9°0'0"N
7°0'0"N
A
-1000
-200
0 50 100 km
Isobaths 200 m
Stations A20
Water masses
B
Potential temperature (ESO80, °C)
Salinity (PSS-78)
AAIW
NADW
AABW
36.25
36.5
36.75
37
37.25
σ2
C
Water masses
c.s
u.p
i.p
l.p
c.sl
a.p
Depth (m)
Distance (km)
D
Salinity (PSS-78)
35.2
35
34.8
34.6

Figure 4

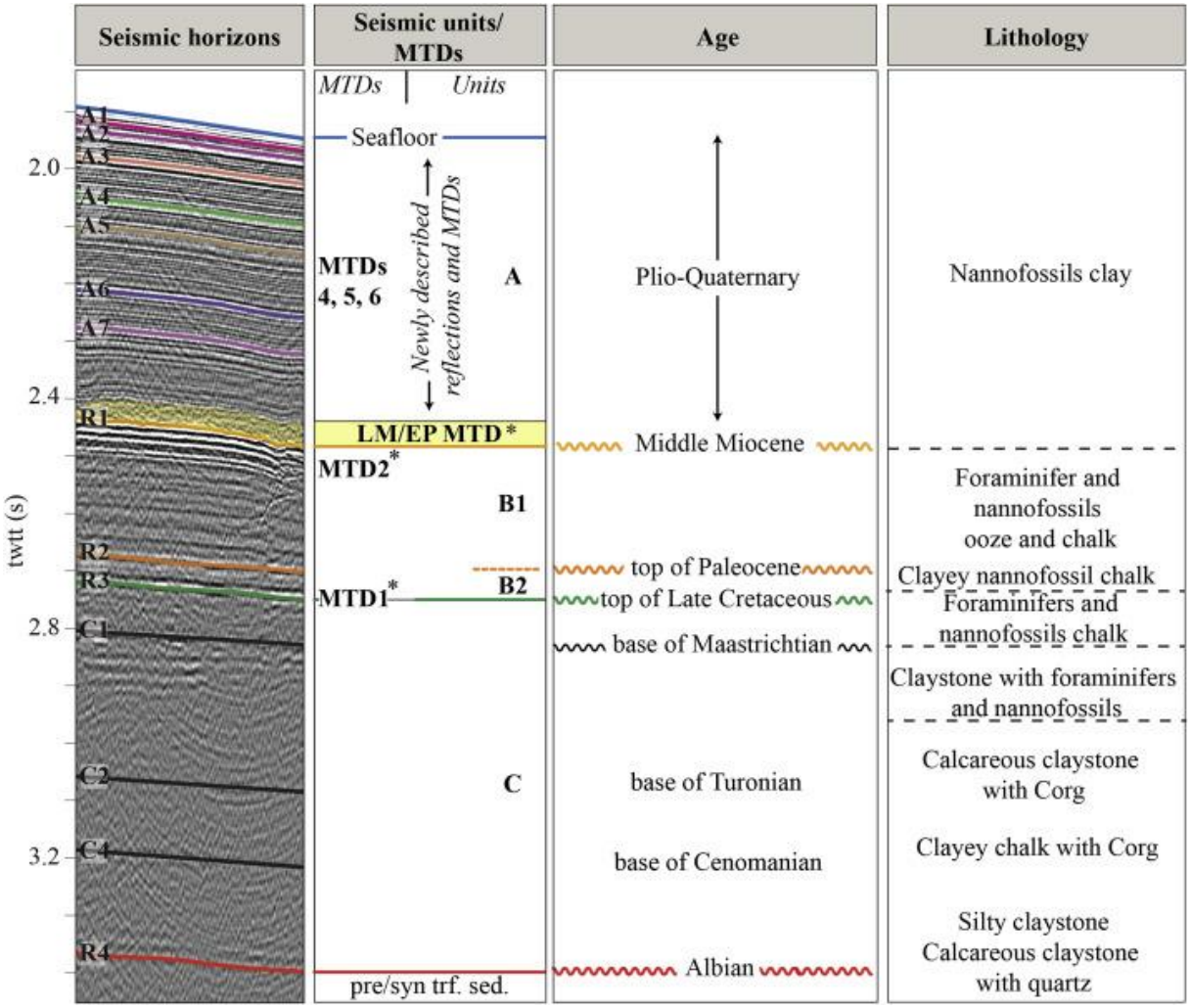
Seismic horizons
Seismic units/ MTDs
Age
Lithology
MTDs
Units
Seafloor
A1
A2
A3
A4
A5
A6
A7
R1
R2
R3
C1
C2
C4
R4
2.0
2.4
2.8
3.2
twtt (s)
MTDs 4, 5, 6
A
Newly described reflections and MTDs
LM/EP MTD *
MTD2*
B1
MTD1*
B2
C
pre/syn trf. sed.
Plio-Quaternary
Middle Miocene
top of Paleocene
top of Late Cretaceous
base of Maastrichtian
base of Turonian
base of Cenomanian
Albian
Nannofossils clay
Foraminifer and nannofossils ooze and chalk
Clayey nannofossil chalk
Foraminifers and nannofossils chalk
Claystone with foraminifers and nannofossils
Calcareous claystone with Corg
Clayey chalk with Corg
Silty claystone
Calcareous claystone with quartz

Figure 5

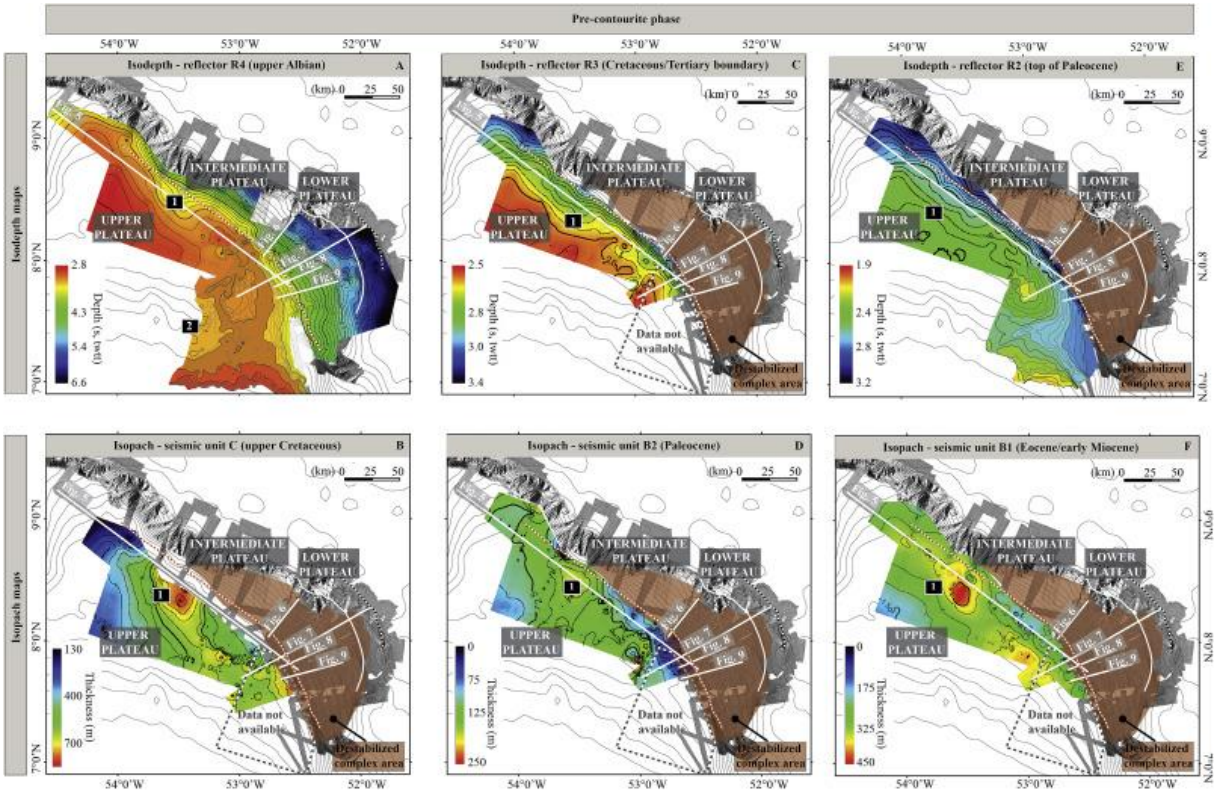

Figure 6

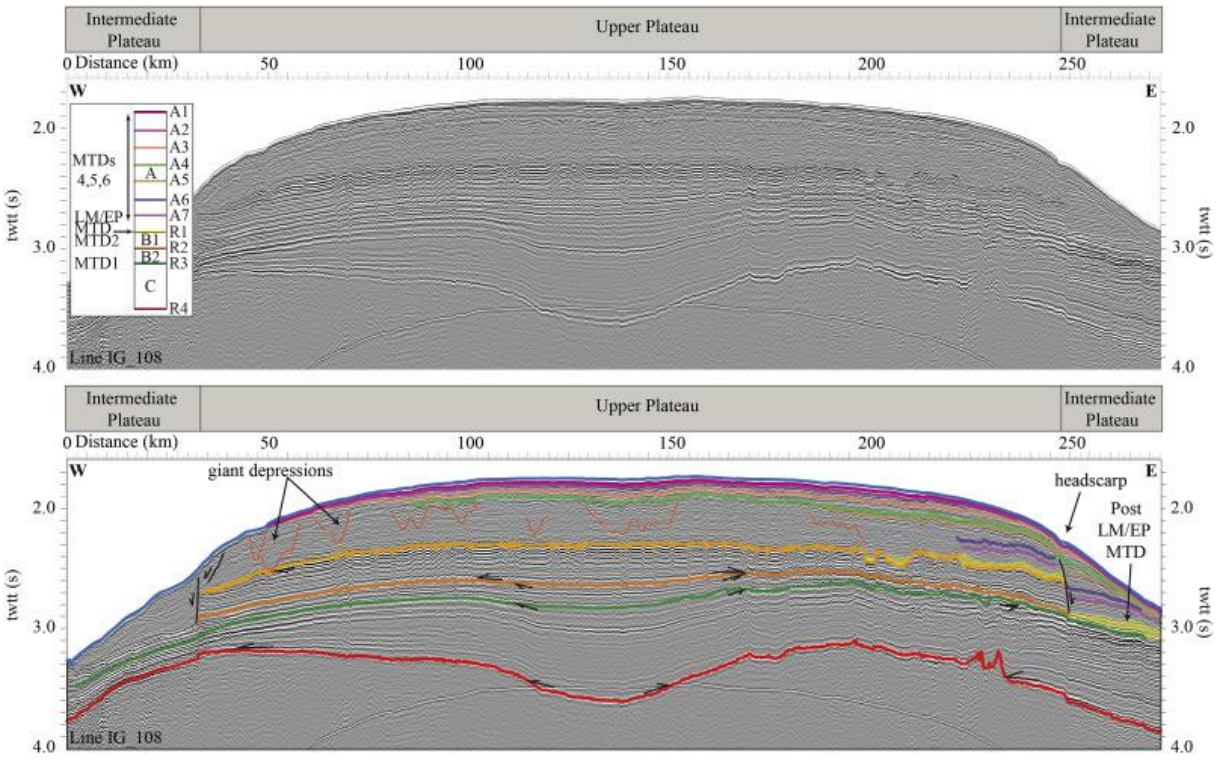

Figure 7

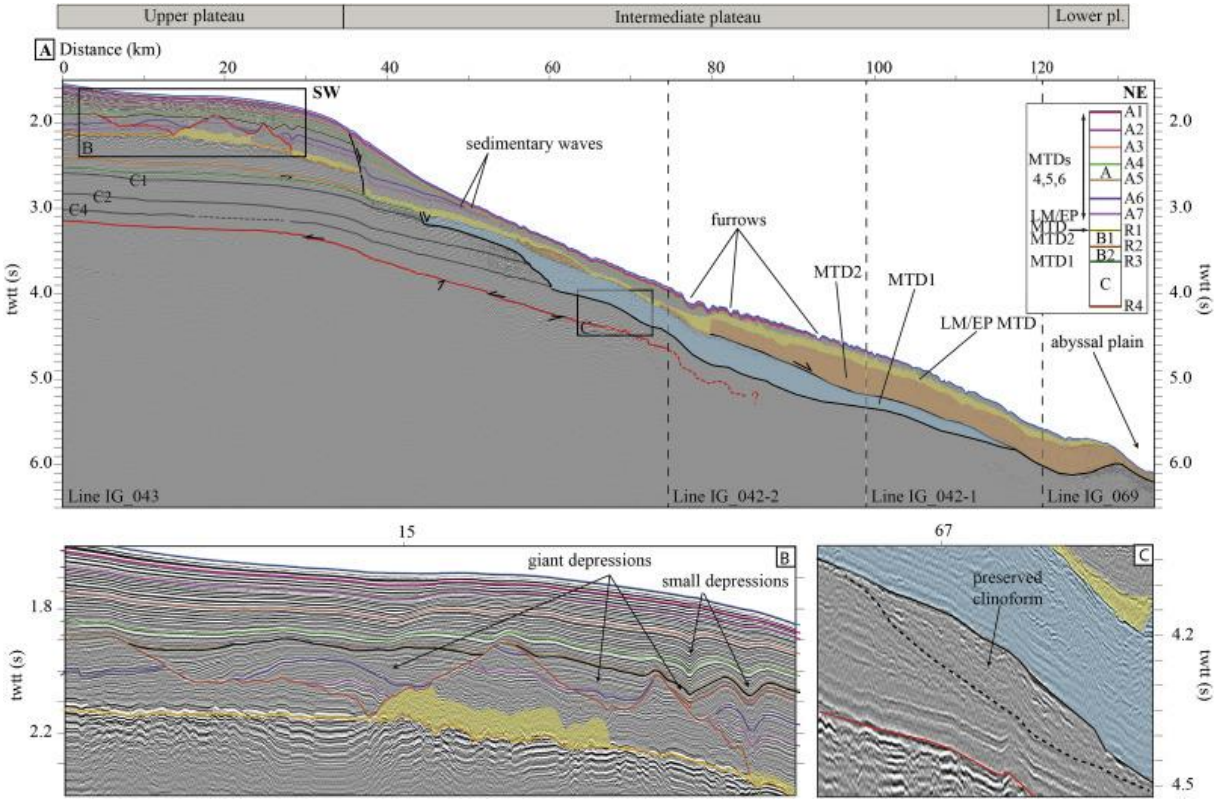
Upper plateau
Intermediate plateau
Lower pl.
A Distance (km)
0
20
40
60
80
100
120
SW
NE
sedimentary waves
furrows
MTD2
MTD1
LM/EP MTD
abyssal plain
MTDs 4,5,6
LM/EP MTD
MTD2
MTD1
A1
A2
A3
A4
A5
A6
A7
R1
R2
R3
R4
B1
B2
A
B
C
C1
C2
C4
twtt (s)
2.0
3.0
4.0
5.0
6.0
Line IG_043
Line IG_042-2
Line IG_042-1
Line IG_069
15
67
giant depressions
small depressions
preserved clinoform
1.8
2.2
4.2
4.5

Figure 8

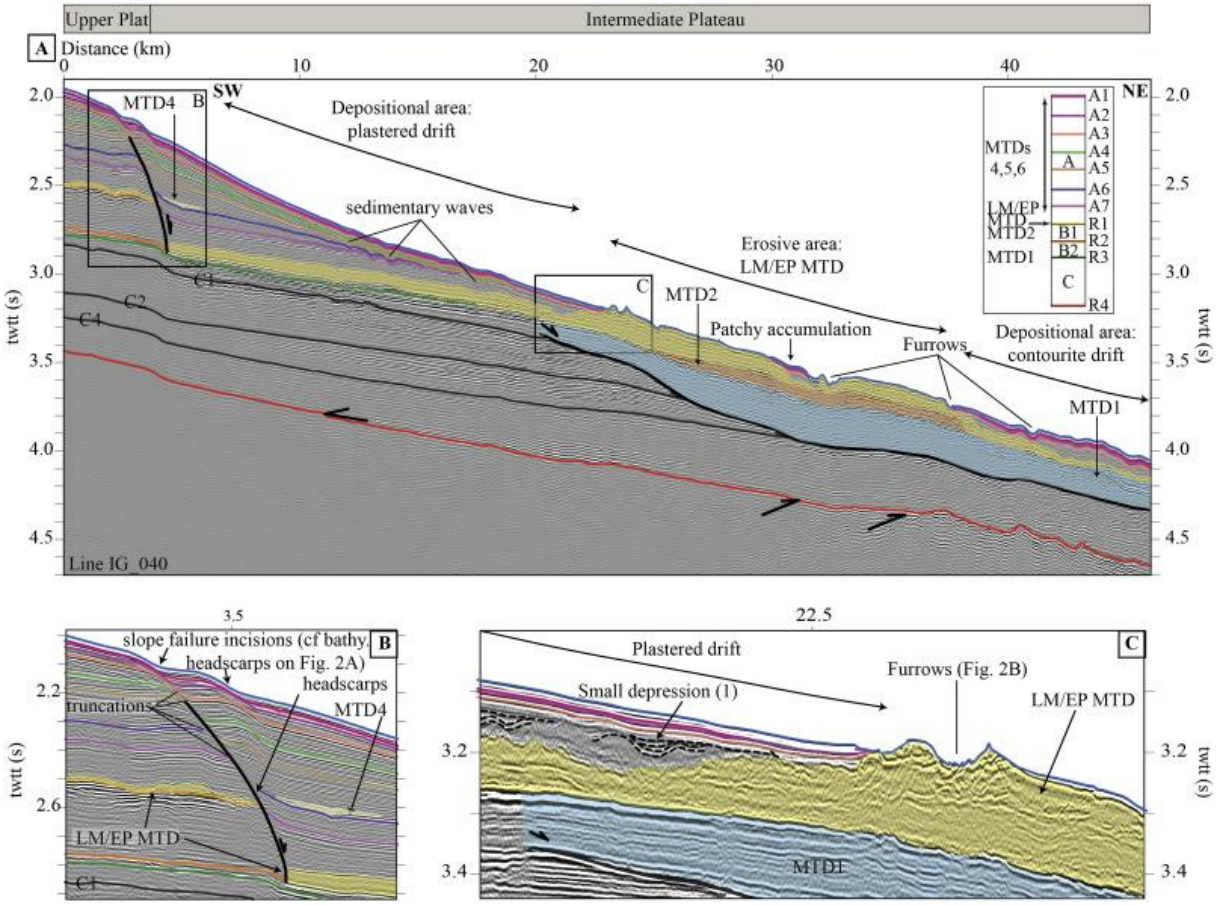
Upper Plat
Intermediate Plateau
A
Distance (km)
0
10
20
30
40
SW
NE
MTD4
B
Depositional area:
plastered drift
sedimentary waves
Erosive area:
LM/EP MTD
C
MTD2
Patchy accumulation
Furrows
Depositional area:
contourite drift
MTD1
C1
C2
C4
MTDs
4,5,6
LM/EP
MTD
MTD2
MTD1
A1
A2
A3
A4
A5
A6
A7
R1
R2
R3
R4
B1
B2
A
C
twtt (s)
2.0
2.5
3.0
3.5
4.0
4.5
Line IG_040
3.5
slope failure incisions (cf bathy.
headscarps on Fig. 2A)
B
headscarps
truncations
MTD4
LM/EP MTD
C1
2.2
2.6
22.5
Plastered drift
Small depression (1)
Furrows (Fig. 2B)
LM/EP MTD
C
MTD1
3.2
3.4

Figure 9

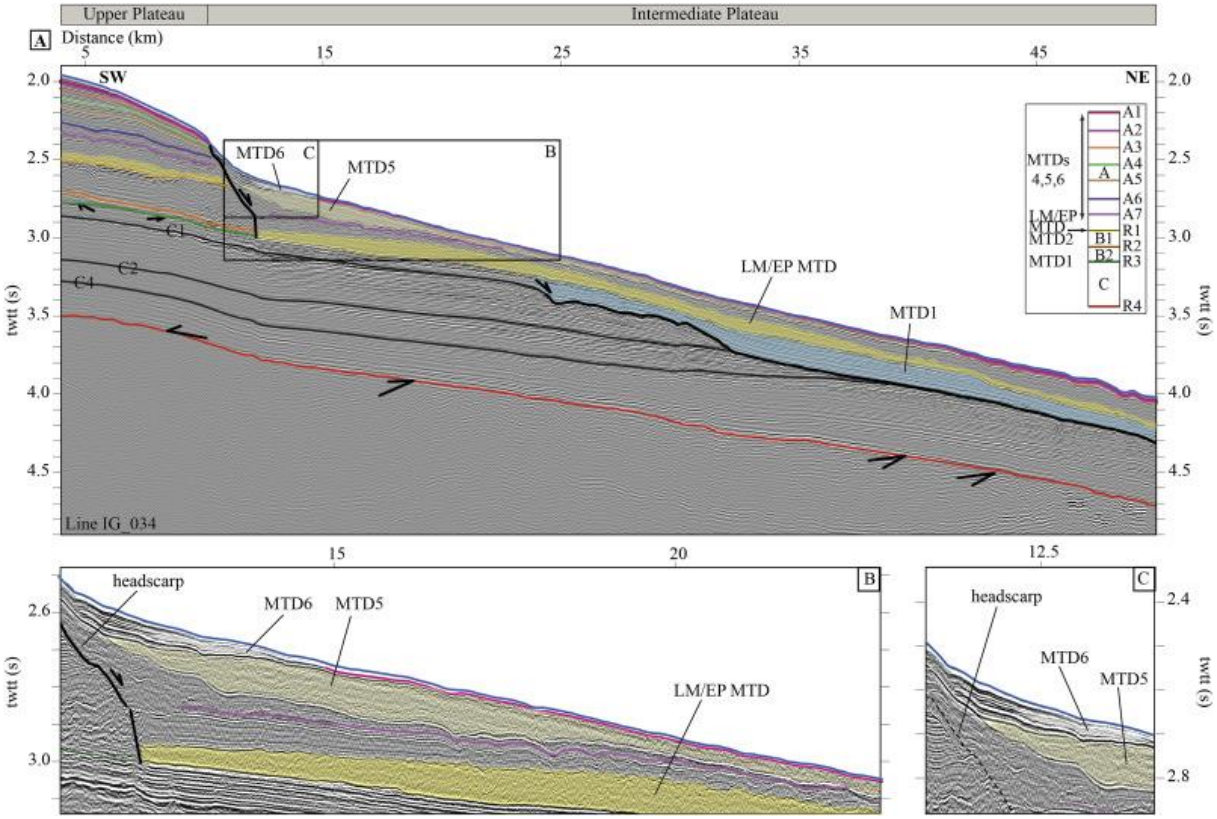

Figure 10